TIDAL INTERACTIONS BETWEEN M81, M82, AND NGC 3077

By

DAVID JOHN KILLIAN

A DISSERTATION PRESENTED TO THE GRADUATE COUNCIL OF
THE UNIVERSITY OF FLORIDA
IN PARTIAL FULFILLMENT OF THE REQUIREMENTS FOR THE
DEGREE OF DOCTOR OF PHILOSOPHY

UNIVERSITY OF FLORIDA

1978

ACKNOWLEDGEMENTS

The extensive computer calculations on which this dissertation was based were carried out on the IBM 370/165 at the Central Florida Regional Data Center (CFRDC), Tampa, Florida, and the Amdahl 470/V6 at the Northeast Regional Data Center (NERDC), Gainesville, Florida. Special thanks for assistance in utilizing the combined CFRDC and NERDC system is extended to C.J. Young, Assistant Director NERDC, and J.G. Schudel, Systems Programmer NERDC.

The author also wishes to thank H.W. Schrader and J.T. Pollock for photographic assistance. Thanks is also due to two people who had a more indirect effect on the completion of this degree: Ms. Eileen Wyman, the author's second grade teacher, who taught the author the value of reading during his protracted childhood illness, and Dr. J.F. Smeltzer, the author's undergraduate advisor, who truly introduced the author to astronomy.

TABLE OF CONTENTS

Abstract of Dissertation Presented to the Graduate Council
of the University of Florida in Partial Fulfillment of the Requirements
for the Degree of Doctor of Philosophy

TIDAL INTERACTIONS BETWEEN M81, M82, AND NGC 3077

By

David John Killian

August 1978

Chairman: Stephen T. Gottesman
Major Department: Physics and Astronomy

The system of galaxies consisting of the galaxies M81, M82, and NGC 3077 is a peculiar system. The principal member, M81, is optically a large beautifully symmetrical spiral galaxy. The other two members belong to the rare and optically unusual IO or IrII class of galaxies, and they are noted for their peculiar structure and stellar distribution. Radio observations have revealed a vast cloud of neutral hydrogen (HI) that envelops all three galaxies, as well as extensive HI bridges connecting the two smaller members of the system with M81.

Numerical models of this system have been made to see if the HI bridges could be products of a tidal interaction between the three galaxies. In such an encounter the gas in the outermost regions would be most heavily affected. Therefore, the galaxies were modelled by rings of massless test particles originally in circular orbits about a central mass. The rings were initially confined to an annular region whose inner radii were approximately the Holmberg radii of the respective galaxies and whose outer radii varied with each galaxy. The central masses were then launched at one another on a predetermined orbit, and the motions of the test particles were followed by integration of the restricted

three body equations of motion. The resulting models were compared for structural and kinematical similarity with the best available observational studies.

The consequences of these models are potentially important in the interpretation of this system of galaxies. The HI bridges can be built tidally, and many of the large scale HI features are duplicated by the models. During the course of the interactions, a large number of particles penetrated the nuclei of the two minor galaxies. If the gas followed similar trajectories, such an event could have precipitated an era of rapid star formation, which in turn could have modified the morphology of the galaxies. The models also indicate that the systemic velocity of M82 is closer to +210 km/sec (heliocentric) and that the orientation of NGC 3077 in the sky is considerably different than that deduced observationally. The position angle of the kinematical major axis of 3077 found in this study was 161° with 3077 inclined 40° to the line of sight (southeast nearest the observer). Though the HI bridges and large scale structures are successfully constructed with the models, the large HI envelope in which the galaxies are immersed is not produced, nor does it appear to be able to be produced, by the interactions. The outer structure of M81 has been modified drastically first by the passage of NGC 3077 approximately 6×10^8 years in the past and then by M82 about 2×10^8 years ago. The outer spiral arm-like features of M81 are probably the result of these modifications.

CHAPTER I

INTRODUCTION

Intergalactic bridges and tails of stellar and gaseous matter are common occurrences in systems of two or more closely associated galaxies. The most widely held theory on the origin of these structures has been that the gravitational forces between the galaxies have raised tide-like distortions in each system and thus drawn out the bridges and tails. The roots of this theory have been traced by Toomre (1974) back to the early part of this century, but the demonstration of the plausibility of the theory awaited the advent of the high speed digital computer.

The gaseous extent of a spiral or irregular galaxy is normally much greater than the corresponding optical image where the bright stellar components and the bulk of the mass currently attributed to the galaxy are located. In this region far from the nucleus, it is reasonable to suppose that gravity is the controlling factor. The gas density is low, minimizing the importance of hydrodynamic effects. Combes (1978), using a typical particle density of 10^{-2} cm^{-3}, estimated the importance of four forces that most reasonably could affect the gas in such regions: the gravitational and magnetic forces of the parent galaxy, gas pressure arising from turbulence in the gas, and self-gravitation of the gas. Considering the force per unit volume of each type, Combes estimated that the magnetic force was an order of magnitude less than that of both the pressure and self-gravitation, which were of comparable size

but in turn an order of magnitude less than the gravitational force. Combes' estimate of the gravitational force per unit volume in a typical bridge in the NGC 4631 group was 3×10^{-34} Nm^{-3}.

Since the gravitational forces of the principal galaxies appear to dominate the gas motions in any galactic tidal encounter, a simplistic model of the encounter can be constructed. The gas may be represented by "massless" test particles in initially circular orbits in an annular region about a central mass. The inner radius of the annulus is large enough to place the innermost particles clearly in the gaseous, non-stellar region of the galaxy where the model is applicable; the outer radius can be determined from observational extent of the gas in the actual galaxy. The circular orbits portray adequately the low dispersion velocities typical of the gas motions in spiral galaxies ($\sim$ 10 km/sec). The motions of the test particles when two such galaxies approach one another can then be followed by numerical integration of the restricted three body equations of motion for each particle. To model adequately the gas, however, a large number of particles in each galaxy are required, necessitating the use of a high speed computer to calculate the motions of the particles.

The system of galaxies consisting of M81, M82, and NGC 3077 exhibits extensive neutral hydrogen (HI) bridges. Observations by Gottesman and Weliachew (1977) and Cotrell (1977) clearly demonstrated that one such bridge appears to connect the principal member, M81, to M82. Cotrell (1976) also found the neutral hydrogen distribution of 3077 to be distorted towards M81, and van der Hulst (1977), working at a higher sensitivity and with a wider range of sampled velocities than Cotrell, found that 3077 also was connected to M81 by an HI bridge. The evidence of

apparent tidal interactions between these galaxies and the fact that both M82 and 3077 belong to the peculiar and rare IrII-IO type of galaxy were considered by Gottesman and Weliachew (1977) perhaps to be related phenomena. They reasoned that the results of a tidal encounter could be to alter violently the gas structure of both M82 and 3077 and thus induce structural changes that transformed the galaxies from normal spirals or irregulars into IrII-IO galaxies.

To test this hypothesis, computer programs were developed to model the system in the previously described manner. The principle aim of the modelling was to see if the observed bridges could be constructed. The secondary aim was to see if any peculiar particle motions or distributions were the result of the encounters. Since the two minor galaxies, M82 and NGC 3077, belong to the structurally unique IrrII-IO class, any unusual gas motions or distributions predicted by the models could have some bearing on the evolution of these peculiar objects.

Details of the construction of the models, orbital considerations, and methods of kinematical and structural comparison of models and observations are detailed in Chapter II. An observational summary of the galaxies is given in Chapter III, and the results of the modelling are discussed in Chapter IV. Chapter V presents the conclusions that may be drawn from the modelling of the system.

CHAPTER II

THE MODEL

The model chosen for this work was a rather simplistic one. Each galaxy was assumed to consist of rings of massless test particles originally in circular orbits in an annular region about a central mass. The central masses were then "launched" at one another on a predetermined orbit. As the masses approached one another, the test particles each experienced an acceleration which, from the restricted three body problem (cf., Danby 1962), can be expressed as

$$\ddot{\underline{r}} = \frac{-GM_1\ (\underline{r} - \underline{r}_1)}{|\underline{r} - \underline{r}_1|^3} - \frac{GM_2\ (\underline{r} - \underline{r}_2)}{|\underline{r} - \underline{r}_2|^3} \quad . \qquad \text{(Eq. 1)}$$

In Equation (1), M_1 and M_2 are the masses of the two central masses, G is the universal gravitation constant, $\underline{r}_1$ and $\underline{r}_2$ are vectors locating the central masses with respect to their center of mass, and $\underline{r}$ and $\ddot{\underline{r}}$ are respectively the position and acceleration vectors of one of the test particles with respect to the M_1-M_2 center of mass (see Figure 1).

To follow the motions of each test particle, one need only integrate the system of equations described above with respect to time from some initial time to some final time. For any choice of orbit, the initial time should be such that M_1 and M_2 are widely separated so that one term of Equation (1) is essentially zero for the particles orbiting each central mass; i.e., Equation (1) reduces initially to the circular

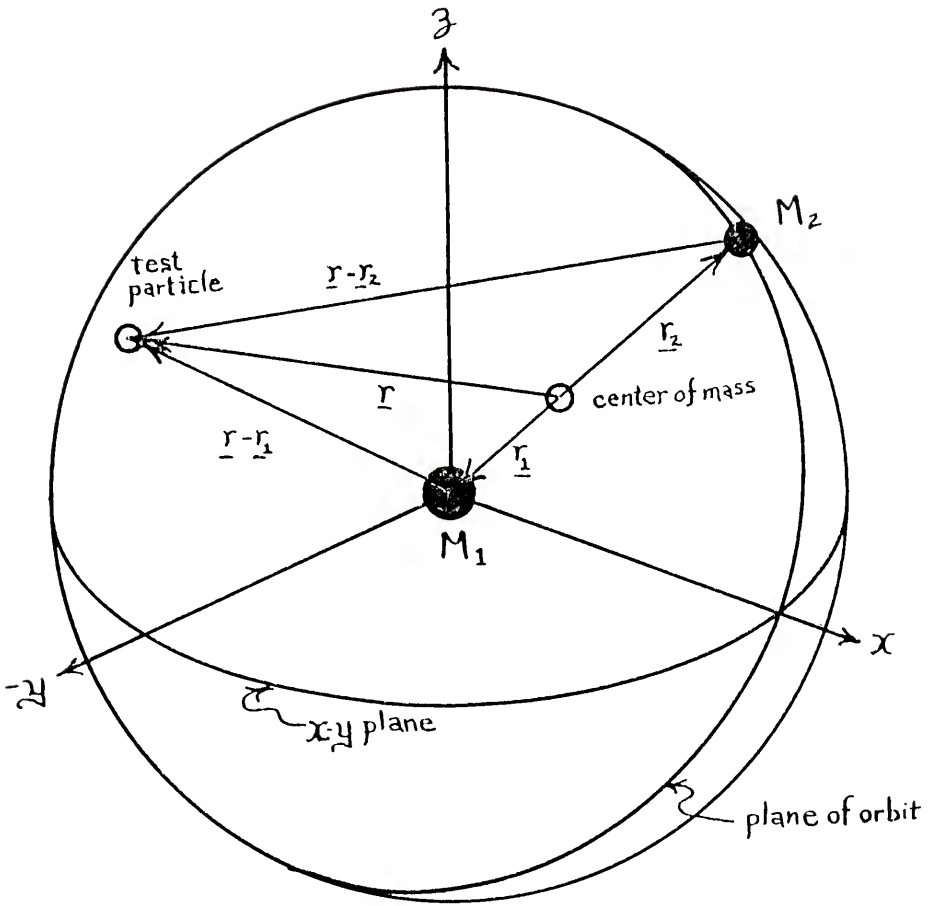

Figure 1. The vector diagram for the restricted three body problem.

centripetal acceleration of the test particles about their central masses. An initial model time of 8×10^8 years before perigalacticon was found to produce adequate separation for the models in this study. The choice of a final time is model dependent and will be discussed later.

The chief difficulty in integrating Equation (1) is that one must constantly evaluate $\underline{r}_1$ and $\underline{r}_2$ as a function of time. If one chooses M_1 as the origin of an arbitrary x-y-z coordinate system as in Figure 1, $R = |\underline{r}_2 - \underline{r}_1|$ can be evaluated from the equations that describe the orbit geometrically; the direction of the vectors comes from the orientation of the orbital plane with respect to the coordinate system. For example (see Danby 1962 for details for all conic section orbits), the separation, R, of the major masses in the case of a hyperbolic orbit is

$$R = (e - 1)^{-1} q (e \cosh B - 1) , \qquad \text{(Eq. 2)}$$

where e is the orbital eccentricity, q is the distance of closest approach, and B is the eccentric anomaly position angle. The eccentric anomaly is related to the time elapsed from the time of closest approach, T, by Kepler's equation for hyperbolic orbits:

$$[C (e - 1)^3 q^{-3}]^{1/2} T = e \sinh B - B , \qquad \text{(Eq. 3)}$$

where $C = G (M_1 + M_2)$. Equation (3) can be solved numerically for B for assumed values of the other parameters, and then Equation (2) may be solved for R, leading to an evaluation of $\underline{r}_1$ and $\underline{r}_2$ from the definition of the center of mass of the M_1-M_2 system.

From this point, the integrations can proceed in any number of ways. For this work, a Fortran IV computer program was built around a

Runge-Kutta integration algorithm developed by Dr. Erwin Fehlberg at the Marshall Space Flight Center. Fifth order Runge-Kutta integrations of Equation 1 were then carried out by high speed computer. Each particle was integrated independently so that the step size used in the integrations could be optimized for it. The results were typically of greater accuracy (6 to 7 significant digits) than could be utilized entirely in the subsequent analysis.

During the course of any integration, however, strict watch must be kept on the denominators of Equation (1). If one of the test particles approaches one of the central masses too closely, the evaluation of Equation (1) is dominated by the term whose denominator is vanishing. At this point, the future behavior of the particle is suspect, and little weight should be given to its future integrations. The motions of such particles could be preserved by regularization of the equations of motion to remove the singularity near each mass (Szebehely 1967), but this was not felt to be necessary for this work. The particles which approached within some limiting distance, r_{min}, of the mass centers during the course of the integrations were simply flagged for future identification. The value of r_{min} was found by numerical experimentation. For any particular central mass, there was a radius within which, for the scale assumed, the calculations were of insufficient precision to maintain circular orbits in an unperturbed situation for the time span of a normal model without some kind of regularization. Therefore, this radius was chosen as r_{min} because all particle motions within it were suspect.

The exact results of any calculation of this type are dependent on several parameters which can be broken generally into two categories. The orbital group determines the behavior of the test particles during

the calculations. The viewing group governs how the results will be compared to the observations.

Figure 2 illustrates these two groups by showing the orbit of M_2 relative to M_1. Mass M_1 is at the origin of an x-y-z coordinate system. The x-y plane is the plane of the test particles initially about M_1; therefore, the initial spin angular momentum of the model galaxy is along the z-axis. The orbit of M_2 about M_1 has eccentricity e, is inclined to the plane of the galaxy by an angle i_g, and has its ascending node on the positive x-axis. The minimum separation of the two masses is q, and this point is located in the plane of the orbit by the angle w_g, the argument of pericenter, which is measured from the ascending node in the direction of motion of M_2. At some time T from closest approach, M_2 is located by the vector $\underline{R}$ from M_1. The direction of $\underline{R}$ depends on angles i_g and w_g which orient the orbit with respect to the x-y plane, but the magnitude of $\underline{R}$ can be found from Equation (2) and from the equation for a general conic:

$$R = q\ (1 + e)\ (1 + e \cos v)^{-1} \quad . \qquad \text{(Eq. 4)}$$

The angle v, the true anomaly, is measured in the plane of the orbit from the position of closest approach to M_2 and is related to the eccentric anomaly, B, in the case of a hyperbola by

$$\cos v = e \cosh B\ (e \cosh B - 1)^{-1} \qquad \text{(Eq. 5)}$$

and by

$$\sin v = (e^2 - 1)^{1/2} \sinh B\ (e \cosh B - 1)^{-1} \quad . \qquad \text{(Eq. 6)}$$

The viewing angles, ϕ and θ, determine how the system would appear to the observer, i.e., how the system would be projected onto the sky. The

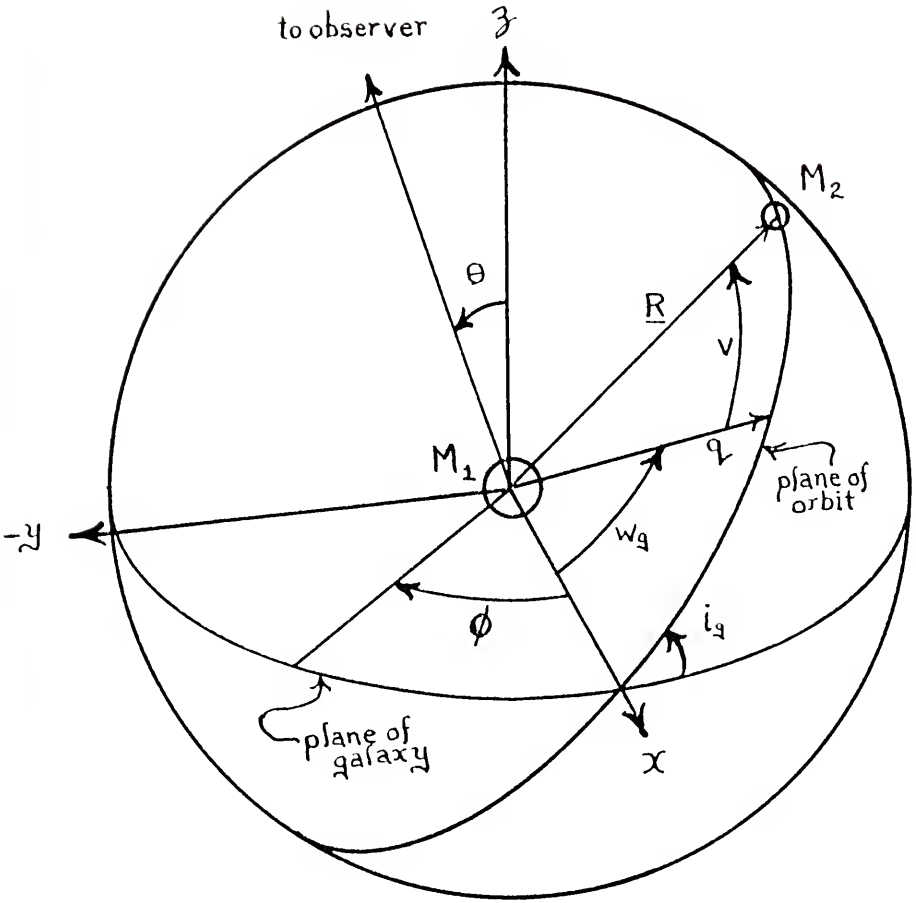

Figure 2. The orbital and viewing angles relative to the plane of a galaxy.

position angle of the line of sight in the plane of the galaxy is ϕ, and the angle θ is the inclination of the line of sight to the z-axis.

Observations can be used to couple the orbital parameters to the viewing parameters. A well-observed galactic system will have the following parameters defined: M_1 and M_2; $\dot{z}$, the relative radial velocity of M_2 with respect to M_1; R_o, the projected separation of M_1 and M_2 in absolute units (if the distance to the system is known, R_o is the distance to the system multiplied by the angular separation of the centers of mass for each system); one of the viewing angles for each galaxy, θ_1 and θ_2, the inclinations of the galaxies to the plane of the sky; and finally, d_o, the position angle of M_2 measured in the plane of the sky relative to the major axis of M_1.

Figure 3 illustrates the orbit in the sky. Mass M_1 again is at the origin, but in this X-Y-Z coordinate system, the X-Y plane is the plane of the sky. Again the ascending node is on the X axis, and R, v, q, and e are as previously defined. However, the inclination i_s and argument of pericenter w_s are now defined with respect to the sky frame.

The problem is geometrically similar now to that of a spectroscopic binary (cf., Smart 1965). In Figure 3, it is clear that

$$z = R \sin (v + w_s) \sin i_s = (R^2 - R_o^2)^{1/2} . \qquad \text{(Eq. 7)}$$

Differentiating Equation (7) with respect to time

$$\dot{z} = \dot{R} \sin i_s \sin (v + w_s) + R \sin i_s \cos (v + w_s) \dot{v} . \qquad \text{(Eq. 8)}$$

As already shown in Equation (4), R is related to v by the equation for a general conic. The conservation of angular momentum in the two body problem relates $\dot{v}$ to R:

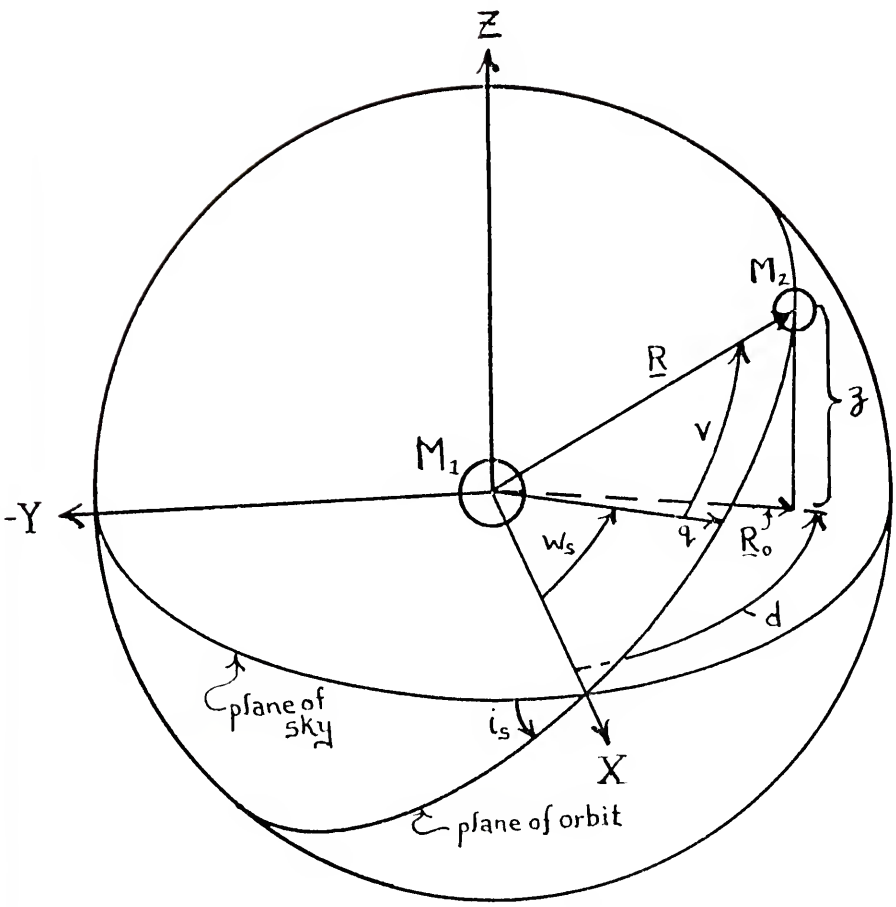

Figure 3. The orbital angles relative to the plane of the sky.

$$\dot{v} = [q\ (1 + e)\ C]^{1/2}\ R^{-2}\ . \qquad \text{(Eq. 9)}$$

Differentiating Equation (4) and substituting Equation (9),

$$\dot{R} = C^{1/2}\ [q\ (1 + e)]^{-1/2}\ e \sin v\ . \qquad \text{(Eq. 10)}$$

Solving Equation (7) for sin i_s,

$$\sin i_s = (R^2 - R_o^2)^{1/2}\ [R \sin (v + w_s)]^{-1}\ , \qquad \text{(Eq. 11)}$$

and substituting Equations (4), (9), (10), and (11) into Equation (8)

$$\dot{z} = \frac{C^{1/2}\ (R^2 - R_o^2)^{1/2}\ [\cos (v + w_s) + e \cos w_s]}{[q\ R^2\ (1 + e)]^{1/2} \sin (v + w_s)}\ . \qquad \text{(Eq. 12)}$$

Therefore, for an assumed set of {e, T, q}, Equation (3), which is a smoothly varying function of B, can be solved by numerical root solving methods for B. Once B is known, Equations (2), (5), and (6) can be solved for R and v. Differentiating Equations (2) and (3), an expression for $\dot{R}^2 + R^2\dot{B}$, the kinetic energy, can be found and evaluated. If R is greater than or equal to R_o and the kinetic energy is greater than or equal to $\dot{z}^2$, Equation (12) can be solved by numerical methods by substituting the values of R and v and treating Equation (12) as a function of w_s only. Over the range $-\pi/2 + v < v + w_s < \pi/2 + v$, Equation (12) is a smoothly varying function which, in the simplest case (v = 0), reduces to the ctn function multiplied by constants. If the value of w_s found from this solution also satisfies Equation (11), the parameter set {e, T, q, i_s, w_s} completely describes an orbit which will fit through the observations.

Figure 4 illustrates the relationship between the orbit with respect to the sky and the orbit with respect to the plane of the galaxy. Once i_s and w_s are known, the angle, d, between the ascending node in the sky and the projected position of M_2 can be found from

$$\tan d = \cos i_s \tan (v + w_s) \quad . \qquad \text{(Eq. 13)}$$

Once d is known, the spherical triangle ABC in Figure 5 can be solved for the values of i_g, w_g, and ϕ necessary to use in the calculations of the particle perturbations and the subsequent projection for viewing. A similar process will yield i_{g2} and w_{g2}, the orbital angles with respect to M_2.

For any set of $\{M_1, M_2, e, T, q\}$, the values of R and the angles v and B are uniquely determined, as described above. However, for exactly the same values of these parameters, variations of i_g and w_g can produce vastly different results for the motions of the test particles. The greatest perturbations occur when the interacting mass, M_2, approaches M_1 in the plane of the galaxy and in the direction of the galaxy's rotation. In this case, i_g is zero, and the orbital and galaxy spin angular momentum vectors are aligned. Significant reductions in the amount of disturbance results when these vectors are anti-parallel. This effect can be illustrated by imagining a particle on the line joining the two masses at the moment of closest approach. In the first case, the particle's rotational motion carries it in the direction of motion of the perturber, effectively increasing the time that the perturbing mass has to accelerate it. In the latter case, the particle and the perturbing mass are separating in opposite directions and consequently reducing the perturbation time. The perturbation is also reduced as

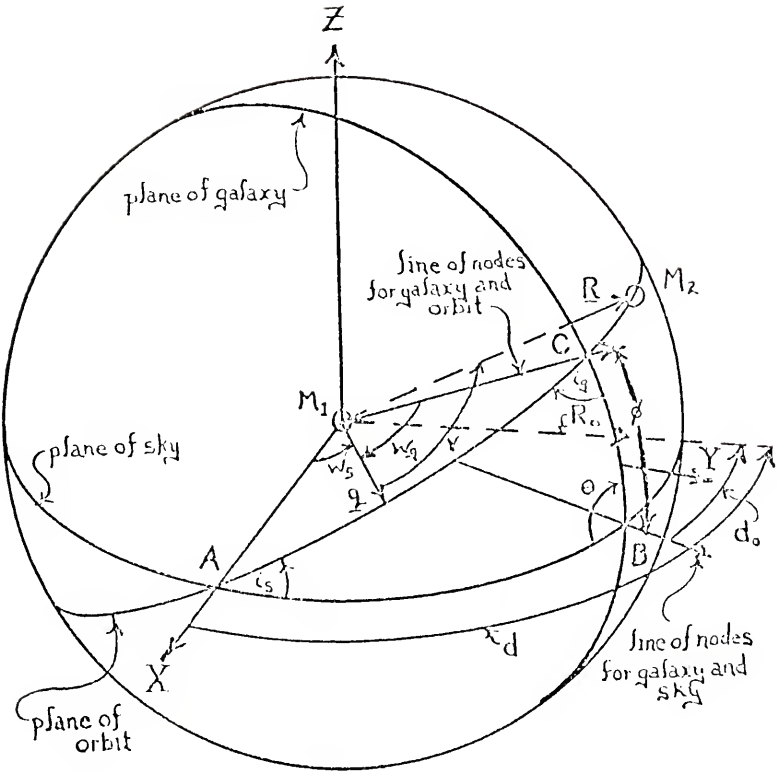

Figure 4. The combined sky and galaxy coordinate systems.

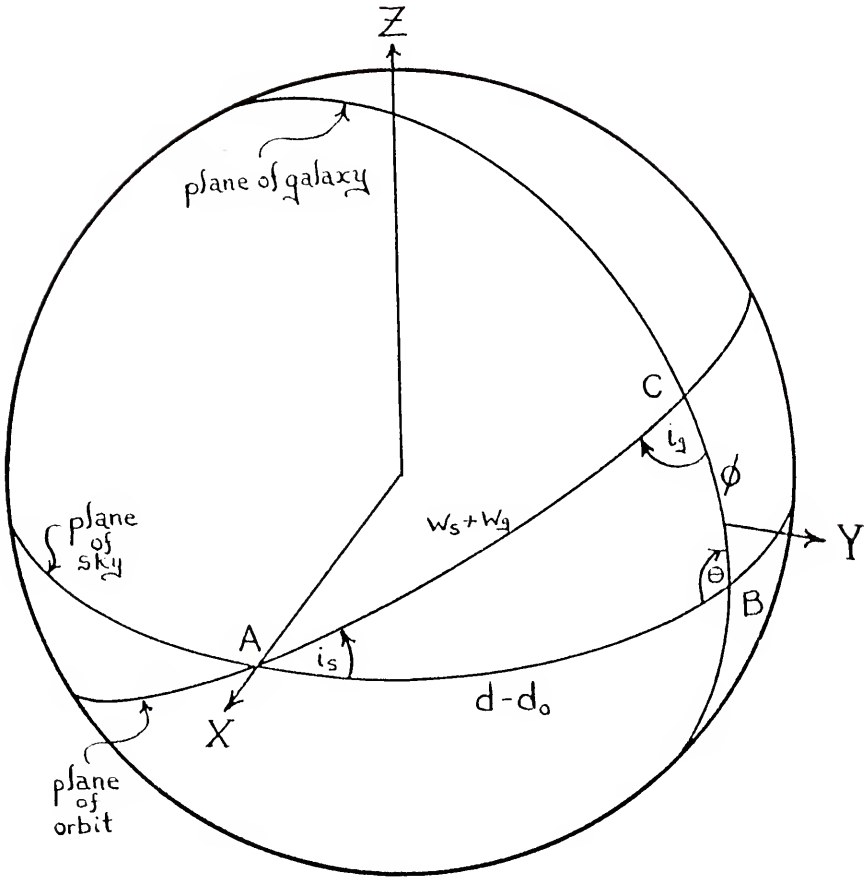

Figure 5. The spherical triangle ABC, which relates the orbital angles in the sky frame to the orbital and viewing angles in the galaxy frame.

the plane of the orbit becomes more inclined to the plane of the galaxy so that the perturbing accelerations do not act in the same plane as that in which the particles are initially moving. Further reductions in the disturbance can be produced in the case of inclined orbits by letting w_g approach 90°. As w_g increases, the point of closest approach, which is also the point of maximum perturbing acceleration, migrates away from the plane of the galaxy, thereby again decreasing the amount of perturbing acceleration in the plane of motion of the particles.

At this point, the problem becomes much more complex than a spectroscopic binary. For a given set of observed parameters, one can find an infinite number of the sets $\{e, T, q, i_s, w_s\}$ which will satisfy the observations geometrically, and there is no reasonable hope of observationally solving this dilemma as is done in the stellar case. However, since each of these sets of orbital parameters produces a different perturbation of the galaxies, the models can hopefully be differentiated by detailed comparison with the observations, as discussed below. Also, some of the sets can be rejected for a number of other reasons. For example, generally no effects can be noted prior to the first passage of M_2 through closest approach. Therefore, T is virtually restricted to values greater than the first time of closest approach. A lower limit to the eccentricity can be roughly calculated for each q value from energy considerations. The total energy of the M_1-M_2 system is constant; therefore, by summing the kinetic and potential energies, it can be shown that

$$(\dot{R}^2 + R^2\dot{v}^2)/2 - C/R = -C\ (1 - e)\ (2q)^{-1} \ . \qquad \text{(Eq. 14)}$$

The minimum value of the kinetic energy is $\dot{z}^2$ at an actual separation of

R_o, which for a given q, lets Equation (14) be expressed as

$$2q\ (\dot{z}^2 - C/R_o)\ C^{-1} + 1 = e_{min}\ . \qquad \text{(Eq. 15)}$$

If no perturbations of one galaxy are observed within a distance R of the center, numerical experimentation will yield a minimum q for which no perturbations are induced by the interacting mass in a ring of test particles of radius R. Finally, if e is too large, the interaction will take place so rapidly that the perturbations induced will be minimal.

The model galaxies, as previously mentioned, were made up of circular rings of test particles, and initially these rings were confined to an annular region of inner radius R_1 and outer radius R_2. Since the model applies most realistically to regions far from the nucleus of the galaxy where Keplerian motions might be expected to dominate the gas motions, R_1 must be large enough to place the first ring clearly in this region. Arbitrarily, the Holmberg (1958) radius of maximum photographic extent of the respective galaxies was chosen to approximate R_1. It is reasonable to suppose that the bright stellar material and hence most of the mass currently attributed to the galaxies lies within this radius. In the case of M81, however, R_1 was taken as 10 kpc because at this radius irregularities begin to appear in its HI distribution (Gottesman and Weliachew 1975; Rotts and Shane 1975). The outer radius was generally taken to be twice R_1, though in some models the outer radius varied in size in order to duplicate some of the observed features with the models.

Each ring was loaded initially with equally spaced particles. The total number of particles in each ring was proportional to the ring radius, and the same constant of proportionality was used for each ring.

By keeping the angular spacing of the particles initially constant in this manner, it was felt that the effects of the interaction would be more visible, particularly in the outer regions where the perturbations are most severe.

This model was applied primarily to the HI structures of the galaxies involved in this study. In the regions of the galaxies which the models consider, the gas atoms are good physical approximations of the restricted three body test particles. Combes (1978; see Chapter I for a discussion of this work) demonstrated that the gravitational force of the central masses clearly dominates the motions of the gas far from the nuclear regions. Therefore, where surveys of the kinematics of the extended hydrogen structure of an interacting galaxy pair exist, direct comparison of the model to the observations is possible. For structural similarity, one would hope to find the final projected particle distribution conforming well to the observed distribution of the gas. For kinematical similarity, one can compare the radial velocity distribution of the particles within a given area to the corresponding radio spectra of the area.

If the model represents the gas motions correctly, one would expect to see good correspondence between the gas distribution at a given radial velocity and the particle distribution at that same velocity. In this work this was accomplished by numerically sweeping a "beam" the size of that used in the observations across the projected particle distribution. The beam could be gated to accept radial velocities only within certain limits, and the positions of beams which contained the appropriate particles were plotted for positional comparison to similar single channel maps of the actual system.

Naturally, discrepancies between the predictions and the actual observations will occur. Little information generally exists, particularly in highly disturbed systems, about the gas distribution prior to the interaction. Spiral structure in disc systems, for example, normally has an associated HI concentration, but such a distribution can not be imposed on the particle distribution of the model without fear of introducing some sort of spurious effect on the model since the orientation of the spiral structure at the time of the encounter cannot be reasonably assumed. The encounter could also produce conditions in the gas where the effects of turbulent gas pressure and self-gravitation of the gas are no longer negligible as the model assumes. If there are significant gas motions in the systems not due to gravitational forces assumed by this model, these, too, would cause the model kinematics to differ from the observed kinematics. Besides such intrinsic effects, instrumental variations in sensitivity and resolution can alter the observed extent of the gas and the amount of detail seen at any particular frequency.

With these complexities in mind, the best course of action appears to be to assume an initially smooth distribution like this model and to look for general trends instead of specific reproduction of the small scale observational details. Therefore, the final model one chooses is not an absolutely unique model, but one that represents the system well geometrically, structurally, and kinematically in comparison with the observations according to some criteria. The criteria used for this work were simply to make the shape of the final particle distribution conform well with the extent of the observed HI structure and to make the radial

velocity distributions of the particles conform well with the extent of the observed gas at particular velocities.

The use of this type of model for the large scale gas dynamics in galactic interactions is not unusual. The first use of it can probably be traced to Pfleiderer and Siedentopf (1961) and Pfleiderer (1963) in which it was used to show that transient spiral structure can arise from tidal interactions in strictly planar encounters. Wright (1972) used a similar model to study the types of structures possible from these interactions of the orbital parameters for strictly planar elliptical orbits. Eneev et al. (1973) and Yabushita (1971) did similar work for hyperbolic orbits, and Yabushita (1977) used this model to study the possibilities of the formation of galactic binary systems after a close passage of two galaxies. These post-Pfleiderer authors were all interested in the production of galactic bridges and tails instead of spiral structure. Toomre and Toomre (1972) applied the model to several extragalactic systems and successfully modelled the structures of M51, Arp 295, NGC 4676, and NGC 4038/39. The important requirements for galactic bridge and tail formation found by these studies were summarized by Toomre (1974): the encounters must be close, the masses must be unequal, and the relative velocities of the galaxies during the close approach must be small.

Attempts have been made to treat galactic tidal interactions in a more complex manner. Clutton-Brock (1972) used a multi-term potential function to calculate the motions of the test particles. However, Clutton-Brock discovered that this innovation for mimicking self-gravitating particles led to the production of diffuse bridges and tails, instead of the generally observed thin filaments. Clutton-Brock reasoned

that the self-gravitating model could perhaps reflect the motions of the stars in a perturbed galaxy, but that the gas motions were best represented by a model with low velocity dispersion of the particles, i.e., rings of particles in a fixed potential field. Tashpulatov (1970a, b) attempted a more hydrodynamic approach. His model galaxies consisted of homogenous prolate ellipsoids, but he worked under the rather artificial constraint that mass could exit the system only at the vertices of the ellipsoids. However, he did demonstrate that bridges and tails could be produced for a wide range of masses and distances of close approach. Neither of these more complex approaches have demonstrated applications to actual systems, and the success of the Toomre and Toomre models clearly argues in the favor of the simpler model used by this project.

Some users of this type of model have tried to make the initial particle distribution correspond more nearly with the current concepts of galactic structure. For example, van der Hulst (1977) modified the gravitational potential of each central mass to the form $-GM\ (r^2 + a^2)^{-1/2}$ where G is the gravitation constant, M is the mass of the galaxy, r is the distance of a point from the center of the galaxy, and a is a constant called the softening parameter. This modification achieves two things. For r less than a, the circular orbital velocity increases more or less with r, much like the rotation curves of many spiral galaxies do in the inner regions. Also it simplifies the integrations by preventing the denominators of Equation (1) from vanishing as r approaches zero. Combes (1978) used a similar approach but used three such potentials to represent the gravitational field in different radial zones from the central masses. In this manner, Combes tried to account for the

gravitational effects of a massive, spherically symmetric galactic stellar halo as well as the optical disc and forced the initial particle distribution to reflect the observed rotation curve of the galaxy. Combes also allowed the population of the rings to decrease exponentially with increasing ring radius to reflect the assumed distribution of mass in the galaxies.

These attempts to reflect "reality" may be questioned on several grounds. In interacting systems there is some question that the observed rotation curve actually reflects the rotation curve of the unperturbed galaxy. Particularly in the region in which the model is applicable, extensive perturbation of the gas can be expected; therefore, imposing the observed rotation curve on the particle distribution may be as artificial as imposing a spiral structure on it. The introduction of the parameter a and the mass of a galactic halo only add more variables to an already complex problem. Particles which enter the interior of the galaxy at which the modified potentials are effective have already left the region in which the model may reasonably be applied. In order to get a reasonable number of particles in the exterior rings for the perturbations to be easily visible, an exponential variation of the number of particles, while perhaps reflecting the variation of mass in the galaxies, dramatically increases the total number of particles, and thus the total computation time. Since the model can at most reflect general trends, these modifications are felt to introduce unnecessary complexity and length to the calculations.

CHAPTER III

THE GALAXIES

The three galaxies involved in this study, NGC 3031 (M81), NGC 3034 (M82), and NGC 3077 are members of the M81 group in Ursa Major, one of the closest groups of galaxies to our own. De Vaucouleurs (1975) described this group as consisting of a few large late type spirals and irregulars and a large number of smaller dwarf systems scattered over an area 40° x 20° in the sky. Tammann and Sandage (1968) placed the distance to this group at 3.25 Mpc, which will be adopted as the distance to the principal member of this group, M81, for this study.

The Galaxy M81 (NGC 3031)

M81 ($\alpha_{1950.0} = 9^h51^m30^s$; $\delta_{1950.0} = +69°18'$) is a large, beautiful, early type spiral galaxy (see Figure 6). Holmberg (1958) classed it as a Sb type system and gave its optical dimensions as 35 x 14.4 arcmin. It has an integrated spectral type of G3 (Humason et al. 1956) and can easily be resolved into stars and HII regions (Sandage 1961). Morgan and Mayall (1957) and Morgan (1958) found M81's blue-violet spectral region to be dominated by light characteristic of K-type giants and therefore classed it as a k-type spiral. Extensive photometry by Brandt et al. (1972) revealed that the spiral arms could be optically traced to within 3 arcmin of the nucleus.

Figure 6. The galaxy M81 (NGC 3031), as photographed with the University of Florida .75 m telescope at Rosemary Hill Observatory. Photograph was provided by Dr. A.G. Smith.

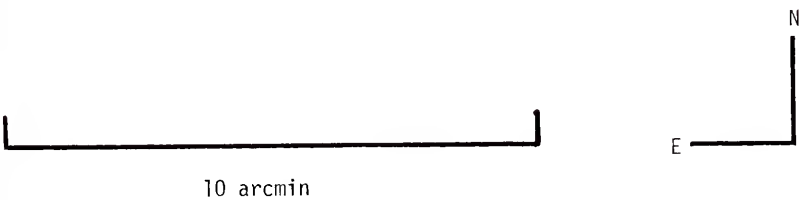

The galaxy has been extensively studied for its geometrical parameters and systemic velocity, both optically and in the radio spectrum. Rotts (1975) has tabulated the results of the studies to date, and general agreement exists on all parameters. For this study, an inclination of 58° and a position angle of the major axis of 151° (Gottesman and Weliachew 1975) will be assumed to describe the system geometrically in the sky. A systemic velocity of -40 km/sec (Rotts 1975) will also be adopted. According to de Vaucouleurs (1959) the southwest side of the galaxy is the nearest to the observer.

Roberts' (1972) HI observations with a 10 arcmin beam revealed that M81 was immersed in a vast cloud of hydrogen distorted in the directions of its two nearby companions, M82 and NGC 3077. Higher resolution studies by Gottesman and Weliachew (1975) and Rotts and Shane (1975) have revealed a wealth of HI data. Both studies have shown an excellent correspondence between the peaks of the HI distribution and the optical spiral arms. Both found a neutral hydrogen density depression at the nucleus of the galaxy. They also found a well-behaved rotation curve for the galaxy from the nucleus out to about 10 kpc from which they deduced a systemic mass of approximately 10^{11} solar masses. Beyond 10 kpc the regularity of the system breaks down. There is evidence of a local depression of neutral hydrogen mass surface density, the appearance of two new outer spiral arm-like features different from the inner spiral arms, and a marked discrepancy between the northern and southern rotation curves (Rotts 1975). Gottesman and Weliachew (1975) and Rotts (1975) felt these outer region differences were due to possible interactions tidally between M81, M82, and NGC 3077.

M81 has been observed in many other spectral regions as well. Kleinman and Low (1970b) listed it as one of their sources of extragalactic IR emission. The disk of the galaxy but not the spiral arms is detectable at 4.8 GHz, as well as a nuclear source (von Kap-herr et al. 1975). At 1.415 GHz, van der Kruit (1975) found the nuclear source as well as the spiral arms, remarking that the northern arms appeared twice as bright as the southern ones. The nuclear source is variable on a time scale of a month (Kellerman et al. 1976; Crane et al. 1976; de Bruyn et al. 1976), and there is evidence for nuclear kinematics quite different from those of the disk (Goad 1976). Geldzahler et al. (1977) believed that the nuclear source was a compact object similar to those found in other extragalactic systems.

Besides its two major companions, M81 has at least two accompanying dwarf systems. One is an apparently spheroidal system 29 arcmin south of the M81 nucleus, and the other (DDO 66) is an irregular 10 arcmin to the east. Both have been resolved and have a maximum extent of about 4 arcmin in diameter (Bertola and Maffei 1974).

The Galaxy M82 (NGC 3034)

M82 ($\alpha_{1950.0} = 9^h51^m54^s$; $\delta_{1950.0} = +69°56'$) is the archetype of its own group of irregular galaxies (see Figure 7). The fusil shaped, dust curdled image of this galaxy has been classed by Holmberg (1958) as an IrII and by de Vaucouleurs and de Vaucouleurs (1964) as an IO. The IrII-IO class of galaxies is characterized by red color, dust, and a smooth luminosity distribution (Chromey 1974a). M82 lies approximately 37 arcmin north of the M81 nucleus, and its turbulent image is not resolvable into stars (Sandage 1961).

Figure 7. The galaxy M82 (NGC 3034), photographed by Dr. A.G. Smith with the University of Florida .75 m telescope at Rosemary Hill Observatory.

Figure 8. The galaxy NGC 3077, photographed by J.T. Pollock with the University of Florida .75 m telescope at Rosemary Hill Observatory.

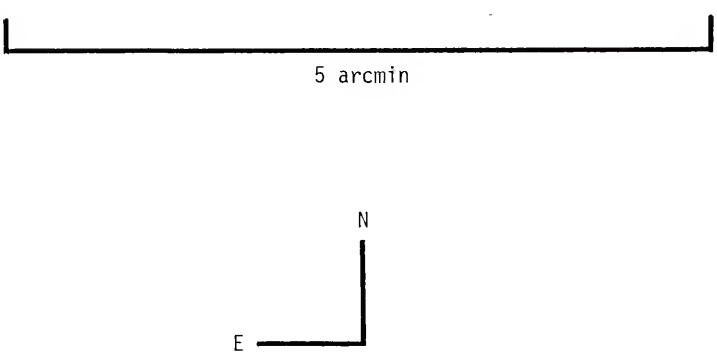

The Holmberg (1958) dimensions of the galaxy are 13.4 x 8.5 arcmin. From this Lynds and Sandage (1963) suggested that M82 was an intrinsic disk system inclined at 8°23' with the northwest side nearest the observer. Heckathorn (1972) placed the optical major axis at a position angle of 64.5°, in close agreement with the direction of alignment of compact radio sources in the nucleus (Kronberg and Wilkinson 1975).

For a nearly edge-on disc system, however, the optical structure of the galaxy is very peculiar. Its smooth non-uniformly illuminated surface is laced with dark absorption lanes. Its A5 type integrated spectral class (Humason et al. 1956) contrasts strongly with its B-V color of +.91 (de Vaucouleurs 1961). Morgan and Mayall (1959) explained this discrepancy by assuming that the galaxy was filled with vast quantities of dust, and indeed estimates of the optical extinction of the hydrogen optical emission lines in the direction of the assumed nucleus exceed 3 magnitudes (Peimbert and Spinrad 1970; van den Bergh 1971).

A system of faint filaments visible in Hα and continuum light also makes the optical image peculiar. The filaments trail out somewhat randomly along the minor axis, reaching a maximum extent of 4 to 5 arcmin from the principal plane. Elvius and Hall (1962) reported that the filaments were highly polarized with the electric vector generally perpendicular to the minor axis and that there was a similarly polarized galactic halo. These results were confirmed by several later studies (Sandage and Visvanathan 1969; Elvius 1972; Schmidt et al. 1976). Though once thought to be rather massive phenomena (Lynds and Sandage 1963; Burbidge et al. 1964), the nature of the filaments is a matter of current debate. Schmidt et al. (1976) showed that the contrast of the filaments is less than 25% above the mean background emission and argued that the

filaments may be nothing more than random collections of efficient light scattering particles. Another peculiar feature of the filaments is the extremely narrow (less than 6 Angstroms) half-width of the polarized Hα emission from them (Visvanathan and Sandage 1972).

The stellar distribution in the galaxy is clearly abnormal for a disk system. In a normal system, HII regions and associations of bright stars are generally confined to the disk and are found rather far from the nucleus. Infrared observations of M82, however, reveal immense HII regions and dozens of knotty structures which are probably young associations of very hot stars, but none are found in the outer regions of the galaxy (van den Bergh 1971). Burbidge et al. (1964) deduced that the sudden switch in integrated spectral type and the switch from an emission to an absorption spectrum with no evident corresponding morphological change as one goes outward from the nuclear regions also indicated a preponderance of early type stars in the nucleus. Peimbert and Spinrad (1970) found significant differences between the size of the Balmer jump and the degree of interstellar ionization between the nuclear and outer regions. Both of these factors they attributed to the presence of a large number of stars earlier than type B1, perhaps thousands more O type stars than exist in our own galaxy. Also, the nuclear regions are an intense source of infrared emission. Kleinman and Low (1970a,b) and Harper and Low (1971) believed that the galaxy's IR luminosity of over 2×10^{44} erg sec^{-1} was due to dust being heated by thousands of O type stars. The presence of these early type, short lived stars in the nucleus probably indicates that the nuclear regions underwent a period of extremely rapid and active star formation within the last 10^8 years (O'Connell and Mangano 1978).

M82 has been heavily observed spectroscopically and in radio emission. Emission and absorption line studies (Mayall 1960; Lynds and Sandage 1963; Burbidge et al. 1964; Heckathorn 1972) reveal a general progression of radial velocities along the major axis attributable to galactic rotation, though peculiar gas motions are evident. Lynds (1961) first identified M82 as the radio source 3C 231. The GHz observations of the nuclear regions (Wilkinson 1971; Hargrave 1974; Kronberg and Wilkinson 1975; Geldzahler et al. 1977; and references in all) reveal a number of compact nuclear sources and a distinct non-thermal nuclear source which dominates the emission. The nucleus has also been detected in HI absorption (Guelin and Weliachew 1970; Weliachew 1974) and is the source of an intense OH maser stronger than any known in our galaxy (Rieu et al. 1977). Rickard et al. (1977a,b) have detected molecular HCN and CO emission from the galaxy. They stated that the CO emission was confined to the optical image and clearly displayed a velocity gradient in the sense of the assumed galactic rotation. They also found that the [HCN]/[CO] ratio was consistent with Galactic values, but the intensity and spectrum of the CO emission implied the presence of large molecular clouds with high interstellar density. For example, Gottesman and Weliachew (1977) quoted a molecular hydrogen content of 10^3 atoms/cm^{-3} to collisionally excite the CO emission. M82's HI emission has been observed several times (Volders and Hogbom 1961; Roberts 1972; Davies 1974; Gottesman and Weliachew 1977; Cotrell 1977). The HI emission structure is clearly distorted from the optical image, and even the rotational component of the kinematics is not particularly prominent (Gottesman and Weliachew 1977). However, it is possible to associate approximately 10^9 solar masses of HI with the optical image (Gottesman and Weliachew 1977;

Cotrell 1977). The details of the HI distribution will be discussed in more detail in a later section.

The systemic velocity of the galaxy is difficult to determine. Results of the optical research to date have been tabulated by Weliachew (1974). The optical research suffers from the fact that there is no clearly defined optical nucleus to use as a reference, and there is no reason to assume in such an unusual system that the center of light and the center of mass are coincident (Burbidge et al. 1964). Radio observations have suffered from the extreme disorder of the system, especially the HI distribution. For example, Volders and Hogbom's (1961) 36 arcmin beam produced a systemic velocity of +184 km/sec which differs extremely from the widely accepted value of +240 km/sec (Heckathorn 1972; Weliachew 1974) derived from optical emission and HI absorption studies. Though Volders and Hogbom's difference can be understood in terms of confusion between the galaxy and the M81-M82 hydrogen bridge revealed in detail by later studies (Gottesman and Weliachew 1977; Cotrell 1977), even the accepted value for the systemic velocity is suspect. Rickard et al. (1977a) found the CO spectrum was symmetrical about a velocity of +206 km/sec. They also found that the CO and HI absorption spectra were broadened the same width, even though the galaxy was optically thin to the CO emission and a much wider velocity range of galactic rotation would be sampled in the CO spectrum. Hence they reasoned that the foreground HI must be undergoing a variety of motions to cause the necessary broadening. Even Burbidge et al. (1964) distrusted the use of their optical emission spectrum position-velocity diagram as a galactic rotation curve and referred their data instead to the Mayall (1960) H and K absorption line rotation curve, hoping the absorption spectrum was arising

in more distant regions free of peculiar motions. O'Connell and Mangano (1978) also pointed out that Heckathorn's (1972) systemic velocity was close to the heliocentric velocity of one of the central bright HII regions not at the nucleus.

Since the rotation curve of the galaxy is so ill determined, the systemic mass is also. However, Burbidge et al. (1964) made some crude estimates based on the velocity extremae of their emission line studies and derived a systemic mass of approximately 10^{10} solar masses. Van der Hulst (1977) attempted to estimate the mass from the mass-luminosity relationship, but the clearly anomalous stellar distribution and heavy obscuration make this procedure questionable. The Burbidge mass would give a HI mass to total mass ratio of about 14% (Gottesman and Weliachew 1977), which would be consistent with the interpretation of the galaxy as a late Sc or irregular (Solinger et al. 1977; Gottesman and Weliachew 1977; O'Connell and Mangano 1978). A mass of 10^{10} solar masses will be assumed to be the mass of M82 for this study.

The explanations of the anomalies of M82 can be grouped into three types: (1) explosive, (2) drifting through dust, and (3) interactive. The objective of the first two types is essentially to explain the polarization of the halo and the filaments. The explosive models (Lynds and Sandage 1963; Burbidge et al. 1964; Solinger 1969) start with some sort of nuclear explosion which ejects matter and vast quantities of relativistic electrons perpendicular to the plane of the galaxy. The polarized emission then arises from synchrotron radiation by the high energy electrons. The initial success of these models led Krienke and Hodge (1974) to propose that there was an explosive subclass to the IrII galaxies. The explosive theories, however, had difficulty explaining

the extremely narrow Hα lines (Visvanathan and Sandage 1972), which led Sanders and Balamore (1970) to propose that the halo polarization rose from dust scattered light from a Seyfert-like nucleus. It now appears that a good deal of the light originates in the disk of the galaxy as well as the nucleus (Solinger and Markert 1975; Schmidt et al. 1978). The dust scattering models (Elvius 1972; Solinger et al. 1977) explained the polarization also by having nuclear and disk light being scattered by dust. However, they required that the dust in the halo be extra-M82 in origin. O'Connell and Mangano (1978) pointed out that dust usually arises in regions of active star formation and that it was difficult to imagine how the necessary amount of dust could be dispersed into the intergalactic medium in a group of galaxies as sparse as the M81 group. They also stated that the dominant scattering component was concentrated to M82 itself and not more uniformly distributed as an exterior cloud might be. The tidal explanations placed all the blame on gravity. The M81-M82-NGC 3077 system has long been known to be immersed in a vast HI cloud (Roberts 1972; Davies 1974). Gottesman and Weliachew (1977) and Cotrell (1977) clearly demonstrated the existence of a HI bridge between M81 and M82 as well as significant irregularities in the HI structures of both galaxies. These authors proposed that the bridge was a direct product of a tidal encounter between M81 and M82 and that the other phenomena were by-products produced by the disruption of the two systems.

The Galaxy NGC 3077

NGC 3077 (see Figure 8) is perhaps the least known of the three galaxies. It lies about 47 arcmin ($\alpha_{1950.0} = 9^h59^m24^s$; $\delta_{1950.0} = +68°58'$)

southeast of the M81 nucleus. Holmberg (1958) placed 3077 among his IrII galaxies also, and he gave its dimensions as 8.8 x 8 arcmin, though Barbieri et al. (1974) found a maximum photographic extent of 10 arcmin. Its amorphous visual image, however, has caused some difficulty in its classification. Van den Bergh (1976) classed the galaxy as an E2p, siding against Holmberg's IrII and de Vaucouleurs and de Vaucouleurs' (1964) IO classification. The detection of a great deal of neutral hydrogen associated with the galaxy has supported the irregular classifications (Lewis and Davies, 1973; Cotrell 1976; van der Hulst 1977).

The geometrical parameters of the galaxy are also difficult to determine because of the lack of a well defined structure. From his HI observations with a single dish, Davies (1974) placed the position angle of the major axis at 60°. The more detailed optical work of Barbieri et al. (1974) placed the position angle at 45°. If the galaxy is an intrinsic disk system, its inclination may be about 45° (Barbieri et al. 1974; Cotrell 1976).

The optical image bears some resemblance to its classmate M82. The central regions are filled with bright condensations visible in Hα light, but there is no well defined nucleus (Demoulin 1969), though one of these sources, asymmetrically placed with respect to the center of light, dominates the emission (Barbieri et al. 1974). Around the central bright region is a generalized halo filled with apparently randomly oriented filaments, arches, and radial lanes as well as several semistellar condensations which may be star clusters (Demoulin 1969; Barbieri et al. 1974). In blue light Barbieri et al. (1974) found a wide absorption lane laced with filaments on the southern border of the strong central source as well as several more bright condensations which did not correspond to

any Hα feature. One of the blue knots, however, corresponds in position with a nuclear 1.415 GHz source detected by van der Kruit (1971).

Spectroscopically the galaxy has long been known as unusual. Seyfert (1943) and Humason et al. (1956) noted it for its broad emission lines and early type spectrum, but Burbidge (1968) demonstrated the galaxy was not of the Seyfert type. De Vaucouleurs (1961) noted that 3077's B-V color of +0.70 made it the bluest of the IO galaxies. Demoulin (1969) and Barbieri et al. (1974) could not find any motions attributable to galactic rotation in their spectral studies. Working from available spectral data, Chromey (1974b) was able to construct a model stellar distribution for the galaxy. He found the system could be best represented by a population composed primarily of solar neighborhood stars and blue globular cluster stars with the young stars concentrated toward the central regions.

Roberts (1972), Lewis and Davies (1973), and Davies (1974) clearly demonstrated the presence of HI associated with the galaxy. An interferometric study by Cotrell (1976) revealed a HI distribution skewed with respect to the optical image and the existence of a narrow HI spike extending over 10 arcmin northward from the main body of the galaxy. More sensitive interferometry by van der Hulst (1977) showed the same features and an HI bridge extending westward from the southern part of the galaxy and seeming to merge with the outer spiral arms of M81. Cotrell (1976) was able to associate 4.1×10^8 solar masses of neutral hydrogen with the main body and the northern spike whereas van der Hulst (1977) found 7.3×10^8 solar masses of hydrogen within the same area. Van der Hulst's southern bridge contained 5×10^8 solar masses of hydrogen. Both Cotrell and van der Hulst proposed a tidal origin for the HI features.

Because of the structural and kinematical confusion in the system, both the systemic velocity and the total mass are not reliably known. The optical systemic velocity of the assumed nucleus found by Barbieri et al. (1974) is -10 km/sec which is also the HI velocity at that position (van der Hulst 1977). However, the centroid of the HI distribution associated with the main body of the galaxy is +15 km/sec from Cotrell (1976) and +10 km/sec from van der Hulst (1977), values consistent with earlier work by Lewis and Davies (1973). Since there is no well defined rotation curve, the mass of the galaxy is equally difficult to estimate. Cotrell (1976) attributed the slight velocity gradient along his assumed major axis to rotation and then calculated a mass of 6×10^9 solar masses by assuming the galaxy was an intrinsic disc system. Van der Hulst (1977) used the mass-luminosity relationship to derive a mass of 10^{10} solar masses. Though both of these parameters are ill-determined, a systemic velocity of +15 km/sec and a mass of 10^{10} solar masses will be adopted for this work.

CHAPTER IV

RESULTS OF THE MODELLING

Following the methods described in Chapter II and the observational constraints assumed from Chapter III, the system of galaxies was modelled in two steps. The first step was the modelling of the M81-M82 system; the second was the modelling of M81-NGC 3077's interaction. No three system models were attempted though the results of the two system models clearly indicate the need for such treatment in the case of M81's outer regions. However, the two system models appear to serve as good fiducial indicators of what the three system effects would be. In the case of M82, the models represented refinements of previously reported work (Killian and Gottesman 1977). The systems were modelled first for an attempted reproduction of the large scale neutral hydrogen features in each. Structural similarity was judged by direct comparison of the maximum shape and extent of the particle distribution to the best available observations of the HI structures. This procedure was applied first to the low mass galaxies, M82 and NGC 3077, whose HI structures have distinctive patterns. Once a satisfactory structure for these galaxies was obtained, the corresponding M81 model was created to see if the observed bridge structures could be reproduced.

If a combined minor galaxy and M81 model passed the structural comparisons, the particle distribution was then examined in detail for position-radial velocity correspondence to single channel maps of the

HI distribution. If the model adequately represents the gas motions induced by the tidal encounter, then good correspondence between the single channel maps and the distribution of the test particles at the corresponding radial velocity should exist.

Two types of comparisons for velocity correspondence were made. First, the distribution of the particles was examined for positional correspondence with the HI features as revealed by the single channel observations. The particle distribution then was "scanned" numerically with a square, untapered "beam" of a size similar to that used by the observers at half beam intervals in right ascension and declination. The beam centers of the beams which contained particles at the desired velocity were plotted as a function of beam position. Beams which contained more than three particles, and thus represented particle "concentrations," were plotted with larger symbols so that the "peaks" of the distribution were accentuated. Intercomparisons between these maps and the observations should also yield good positional correspondence, provided one assumes that the real gas is nearly as optically thin as the particle "gas."

Models which passed both comparisons adequately were then subjected to a variation of the orbital and systemic parameters. In particular, the effects of a different assumed mass and/or a different assumed systemic velocity were studied. Also considered were changes in the perigalacticon, q, and the orbital eccentricity, e.

The modelling results presented here are the end product of over 350 simulations of the systems. These models, though by no means unique, are representative of the best results obtained for structural and velocity intercomparison. They also have some interesting implications

for the structure of the systems before and after the interaction. For easy reference, the systemic and orbital parameters for all the models discussed in this chapter have been tabulated in Table I.

The M81-M82 Models

M82 presented some immediate difficulty in modelling because of the indeterminacy of its systemic velocity. As a result, two modelling lines were followed. Model 1 assumed the systemic velocity of Weliachew (1974) and Heckathorn (1972) of +240 km/sec. Model 2 assumed +210 km/sec as the systemic velocity, a value closer to the CO central velocity determined by Rickard et al. (1977a).

The next difficulty was the orbit itself. Using the above systemic velocities and the assumed masses of M81 and M82, a quick calculation of the kinetic and potential energies of M82 relative to M81 in the plane of the sky at the assumed separation clearly indicates that the total energy is positive and the orbit is therefore a hyperbola. Hyperbolic orbits tend not to produce extensive bridges because of the great velocity at which the perturbing mass moves relative to the other mass during closest approach.

The hyperbolic orbit placed some immediate constraints on the orbit. Since the aim was to build a bridge from M81 to M82, the orbit must be one which maximized the limited amount of perturbations caused by M82; the low mass ratio of M82 to M81 (1/10) and high relative velocity of M82 in a hyperbolic orbit about M81 were not conducive to building bridges. The best cases, therefore, were close, direct (in the direction of M81's rotation) approaches with low inclination with respect to M81 and an argument of pericenter nearly in M81's plane.

TABLE I

MODEL PARAMETERS

	M81 (all)	M82 (Model 1)	M82 (Model 2)	NGC 3077
Total Mass (x 10^{11} solar masses)	1.0*	0.1*	0.1*	0.1*
Apparent Separation from M81 (kpc @ 3.25 Mpc)		35*	35*	44.2*
Position Angle of Major Axis (°)	151*	65*	65*	161
Inclination to Line of Sight (°)	58*	10*	10*	40
Systemic Velocity (heliocentric, km/sec)	-40*	+240*	+210*	+15*
Model Annulus Data				
Inner Size (kpc)	10	4.0	4.0	4.0
Outer Size (kpc)	20	9.5	9.5	7.0
Number of Rings	9	12	12	7
Ring Spacing (kpc)	1.25	0.5	0.5	0.5
Total Number of Particles	540	324	324	154
Perigalacticon to M81 (kpc)		15	15	22.5
Eccentricity of Orbit		3.5	2.9	0.95
Display Time of Model (x 10^{8} yrs) (after Perigalacticon)		2	2	6
Inclination of Orbit in the Sky (i_s, °)		67.6	67.1	58.1
Inclination of Orbit to M81 (i_g, °)		-13.2	-10.1	17.9
Inclination of Orbit to Minor System (i_{g2}, °)		80.9	85.8	-72.6
Argument of Pericenter in Sky (w_s, °)		-23.1	-28.7	-7.0
Argument of Pericenter with Respect to M81 (w_g, °)		18.3	-4.1	89.0
Argument of Pericenter with Respect to Minor System (w_{g2}, °)		52.0	48.6	-178.1
Viewing Angle (ϕ, °)		-43.8	-63.1	-5.3

Note: Orbital and Viewing Angles are as defined in Chapter II. Values marked with an asterisk (*) are adopted or derived from observation; see Chapter III for references.

A limit on the distance of closest approach was provided by observation and numerical experimentation. Rotts (1975) found that at 8 to 10 kpc from the M81 nucleus the symmetry of the inner HI spiral structure began to break down. If this deviation is caused, as Rotts supposed, by the tidal encounter, the model would hopefully produce a disturbance at about 10 kpc. However, since the galaxy is beautifully symmetric within this region, the model disturbance should be minimal closer to the M81 mass center. By numerical experimentation, it was found that a ring of particles at a distance of 10 kpc from the M81 mass center began to be perturbed when q, the distance of closest approach, was approximately 15 kpc. This was taken as the approximate minimum value for q.

A particular structural feature in M82 was also important. Both Gottesman and Weliachew (1977) and Cotrell (1977) found a "spike" of neutral hydrogen rising northward almost perpendicular to the galaxy's major axis at its eastern extremity. This spike is quite prominent in the single channel maps of Gottesman and Weliachew (1977; hereafter called GW), extending over 10 arcmin from the optical major axis. The GW brightness temperature maps also indicate that the northern tip of the spike might be a clump or concentration of gas since the brightness temperature contours of this region are detached from the main body of the galaxy.

The models of M82 characteristically had an s-shaped distortion after close approach to M81, with the body of the s along the galaxy's major axis, the west end pointing toward M81, and the east end pointing northward like the spike. Generally, this northward feature would begin to become evident about 10^8 years after the close approach, growing larger but staying relatively intact until about 3×10^8 years after

close approach when the rotational and peculiar velocities of the particles had dispersed it. This model feature was assumed to be the counterpart of the GW hydrogen spike. Its position and size were used as timing and structure marks in the analysis of the models.

Many parameters affected the development of this spike in the models. If the distance of close approach were too great, the spike would not develop sufficient height. Successive attempts at different q values brought M82 closer and closer to M81 at their minimum separation in an attempt to increase the size of the spike. Finally, the q value reached the 15 kpc limit imposed by the HI structure of M81, but the spike still did not extend to the observed height. At this point, the migration of the minimum separation was halted. The time after perigalacticon was then adjusted within the 1 to 3 x 10^8 year range imposed by the coherence of the spike. A time of 2 x 10^8 years was found to give the greatest height of the spike with the greatest concentration of particles in the spike feature. With T and q fixed at these values, the position angle of the spike could be adjusted somewhat by variation of the eccentricity of orbit which produces a change in the orbital angles of the encounter as explained in Chapter II. In this manner, the best positional agreement between the model spike and the observed spike was obtained. The extent of the spike was then obtained by simply increasing the size of M82, which produced another interesting effect. The outermost rings of this enlarged galaxy rose directly into the spike and were twisted into a clump at the spike's northern tip, a clump suggestive of that in the GW observations. Using the information gleaned from this structural study, the value of q was increased and similar attempts at structural duplication were attempted. However, no significant

improvements were found, and in fact, these more distant approaches made alignment of the model and observational spike very difficult, when it could be done at all.

The best structural results of the M81-M82 models are displayed in Figures 9 and 10, which illustrate the +240 and +210 km/sec systemic velocity models, respectively. The models are quite similar, showing the northern spike as well as a well developed intergalactic bridge. The maps of Cotrell (1977) and GW indicate that the bridge is clumpy, and the models suggest, particularly southwest of M82, that the clumps could be due to an intermixing and/or superposition in the line of sight of materials from both galaxies.

Though structurally similar, the two models differ greatly in the kinematics. Figures 11 and 12 show the particle radial velocity distributions in a 40 arcmin square about M82. In these figures, the particles have been plotted if their radial velocities were within a 21 km/sec "bandwidth" of a given central velocity. The central velocities and bandwidth are those of the GW single channel maps. To aid further in the comparison of the model to the GW maps, the particle distribution was then scanned numerically with a square 4.4 arcmin beam at half-beam intervals. The coordinates of each beam which detected particles within the given velocity range were then plotted. Those beams which contained more than 2 particles were plotted with a larger symbol so that the "peaks" of the distribution's particle density were visible. The results of these scans of both distributions are displayed in Figures 13 and 14. The reader should note that apparent gaps and discontinuities in Figures 11 through 14 between features in the same velocity range could be due to the finite number of points in each galaxy model as well as the calculated effects of the interaction.

Figure 9. Particle distribution for Model 1 of the M81-M82 interaction at 2 x 10^8 years after perigalacticon. Circles denote particles which were initially about M81; M82's particles are marked with asterisks. The large crosses indicate the Holmberg (1958) dimensions of the respective galaxies as well as the assumed orientation of the galaxies. The solid line indicates the orbital path of M82 about M81, and the arrow indicates the perigalacticon with respect to M81's center. The coordinate tic marks are at 10 arcmin intervals from the center of M81.

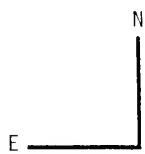

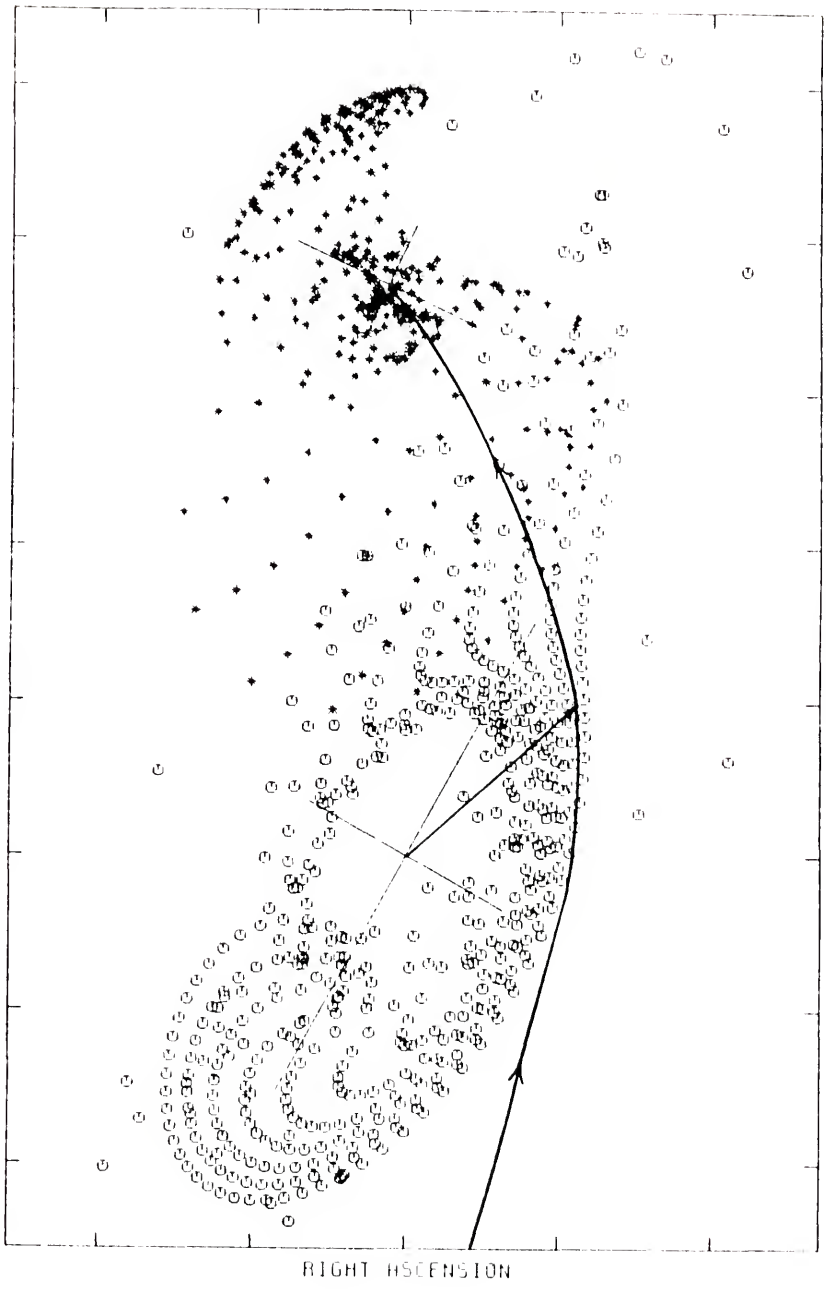
DECLINATION
RIGHT ASCENSION

Figure 10. Particle distribution for Model 2 of the M81-M82 interaction at 2 x 10^8 years after perigalacticon. Plotting conventions are the same as those in Figure 9.

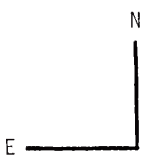

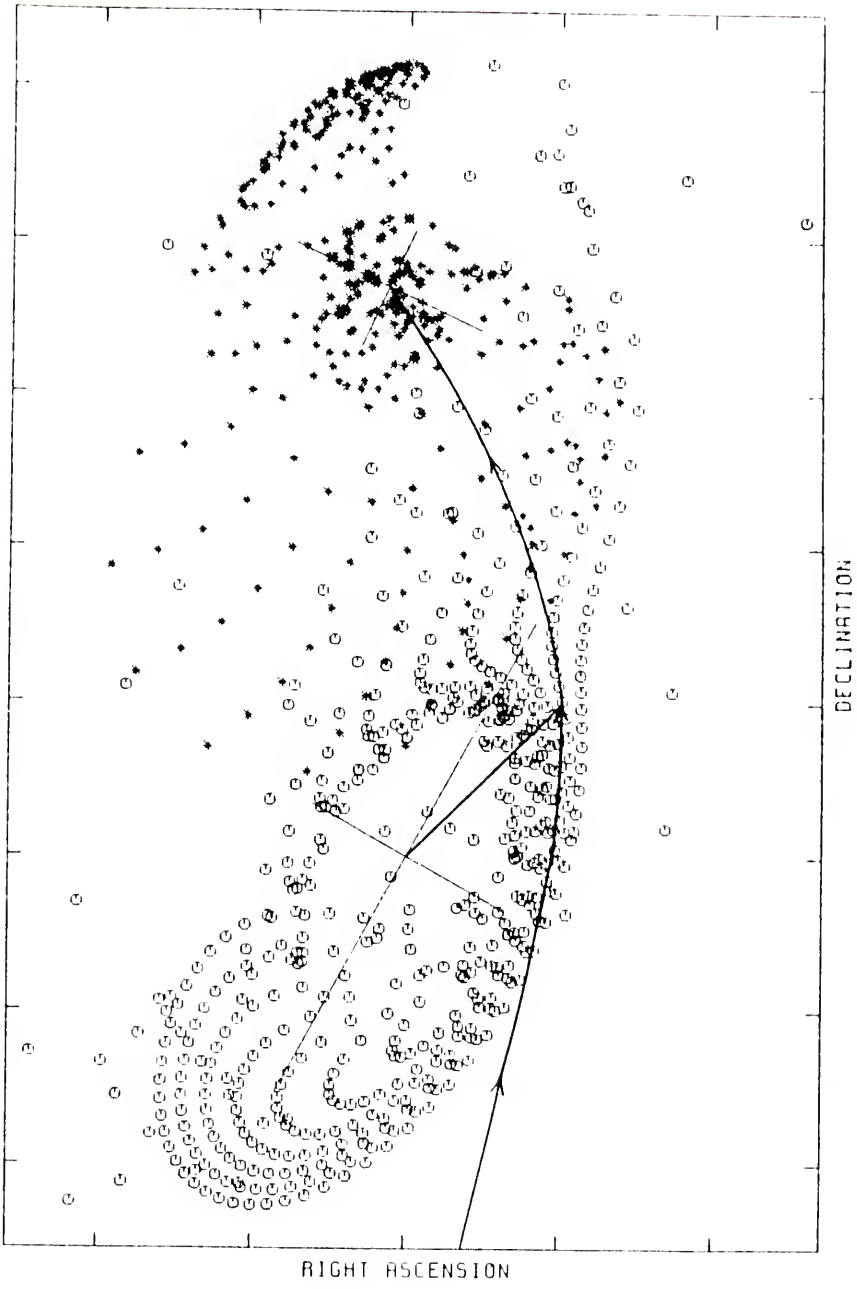
DECLINATION
RIGHT ASCENSION

Figure 11. Radial velocity distribution of particles in Model 1 near M82. Particles were plotted if their radial velocities were within a 21 km/sec bandwidth centered on the velocity listed in the lower left corner of each plot. The cross indicates the Holmberg (1958) dimensions of M82 and the assumed orientation of the galaxy. Coordinate tic marks are at 10 arcmin intervals from the center of M82.

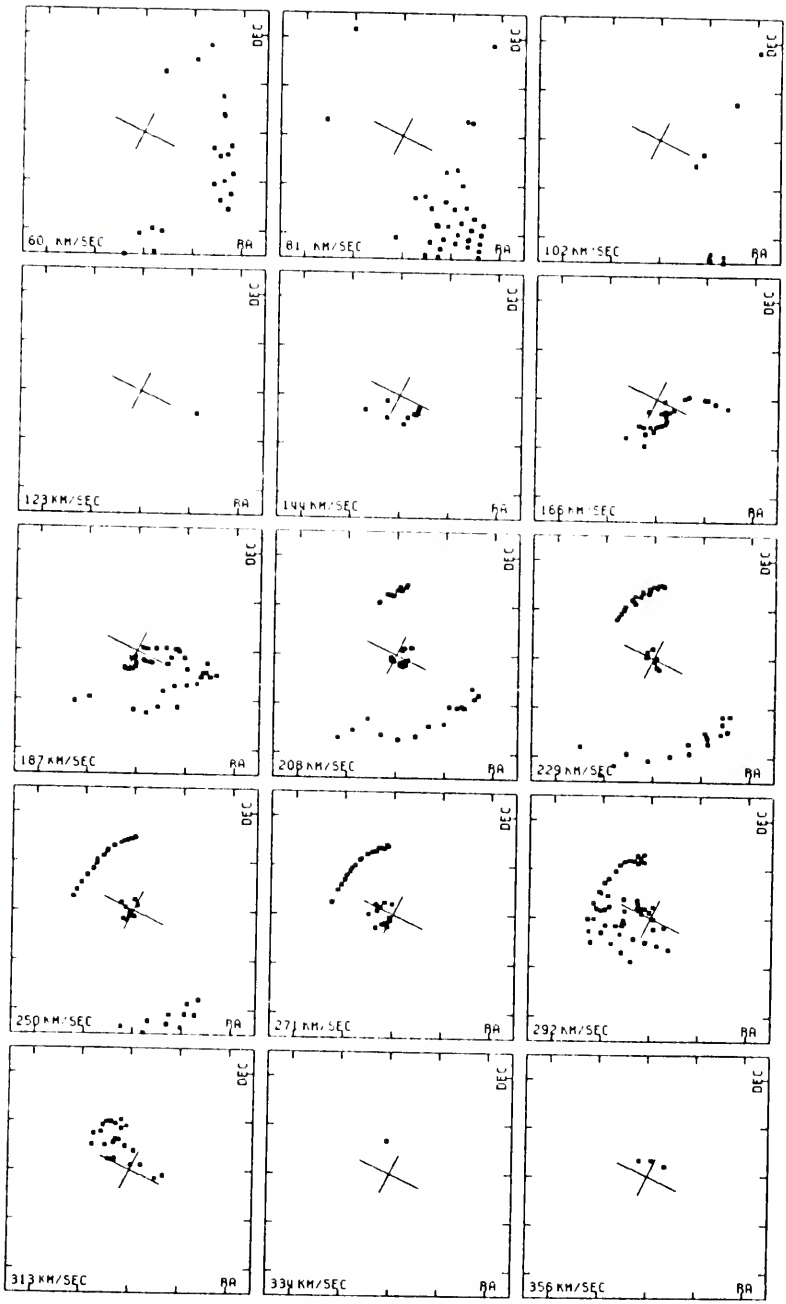
DEC
RA
60 KM/SEC
81 KM/SEC
102 KM/SEC
123 KM/SEC
144 KM/SEC
166 KM/SEC
187 KM/SEC
208 KM/SEC
229 KM/SEC
250 KM/SEC
271 KM/SEC
292 KM/SEC
313 KM/SEC
334 KM/SEC
356 KM/SEC

Figure 12. Radial velocity distribution of the particles in Model 2 near M82. Plotting conventions are the same as in Figure 11.

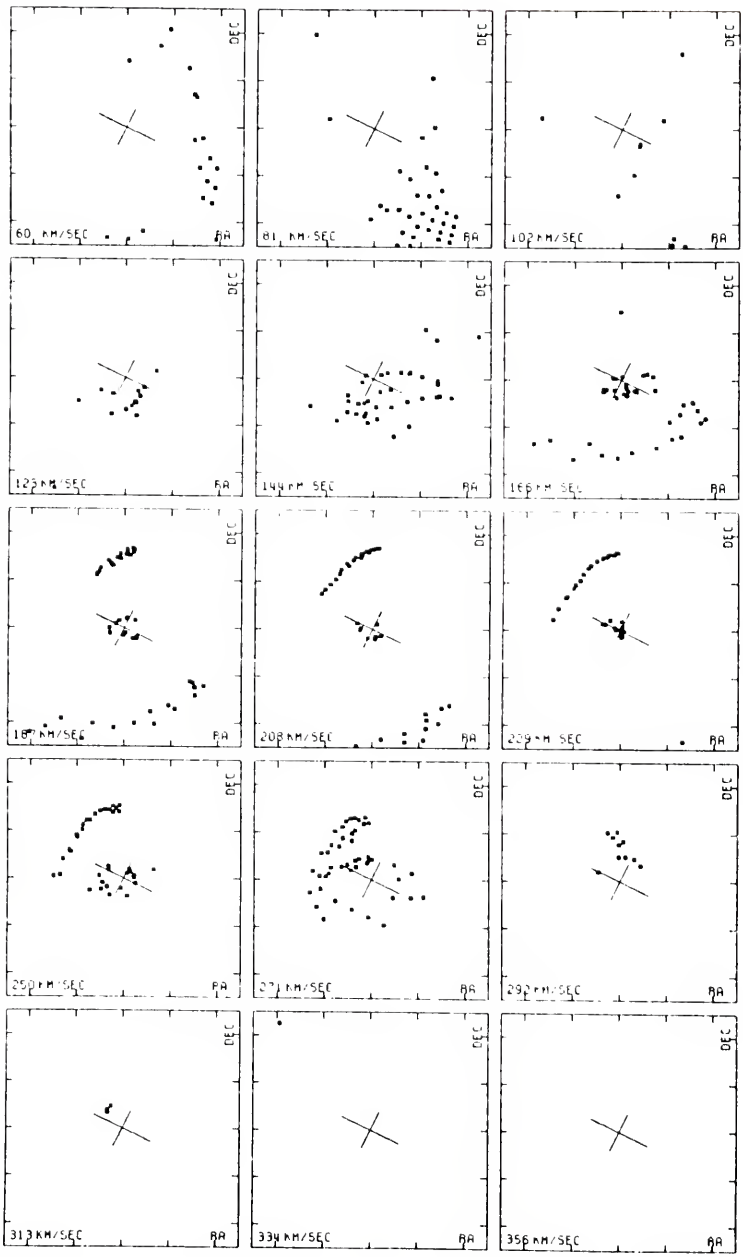
DEC
RA
60 KM/SEC
81 KM/SEC
102 KM/SEC
123 KM/SEC
144 KM/SEC
166 KM/SEC
187 KM/SEC
208 KM/SEC
229 KM/SEC
250 KM/SEC
271 KM/SEC
292 KM/SEC
313 KM/SEC
334 KM/SEC
356 KM/SEC

Figure 13. Beam-smoothed radial velocity distribution of the particles in Model 1. The particle distribution in Figure 11 has been scanned with a 4.4 arcmin square, untapered beam at half-beam intervals in right ascension and declination. If the beam contained a particle, the beam center was plotted. Beams enclosing more than two particles were denoted by plotting the beam center with a larger symbol. Other plotting conventions are as in Figure 11.

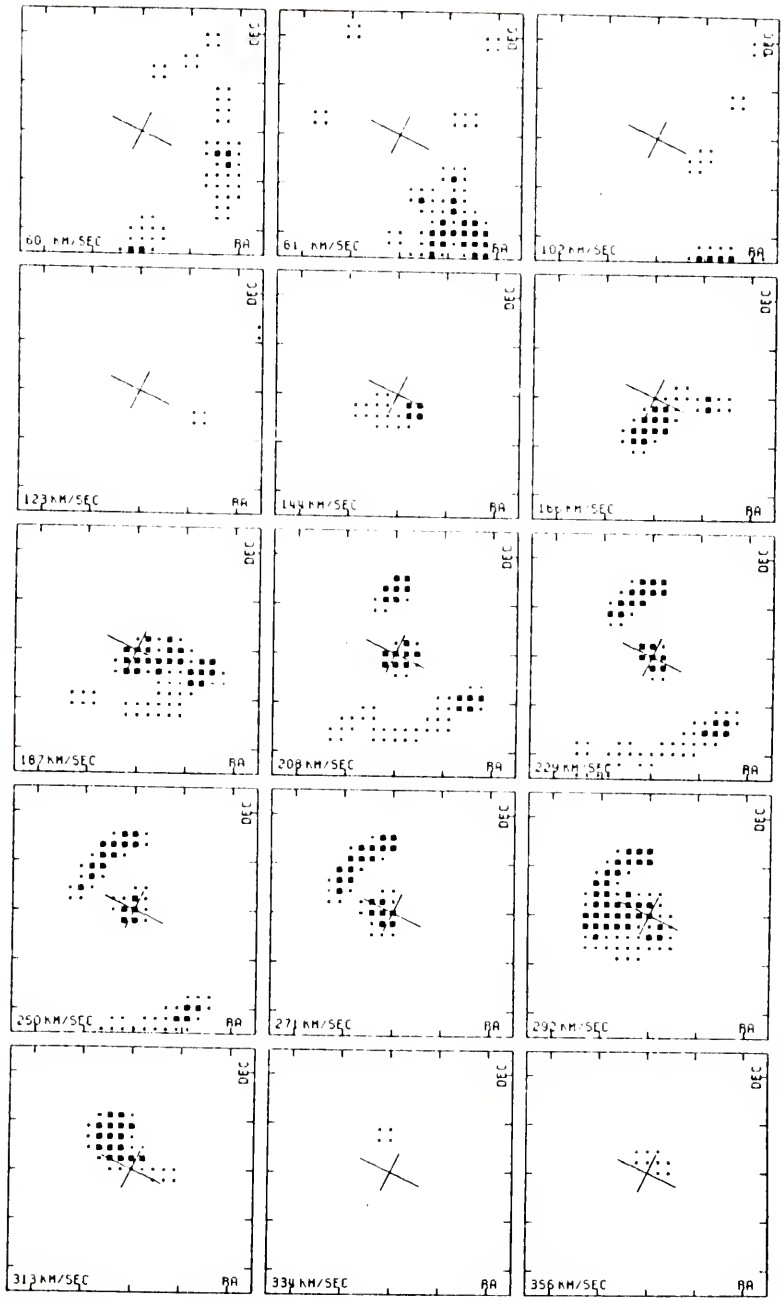
60 KM/SEC
61 KM/SEC
102 KM/SEC
123 KM/SEC
144 KM/SEC
165 KM/SEC
187 KM/SEC
208 KM/SEC
229 KM/SEC
250 KM/SEC
271 KM/SEC
292 KM/SEC
313 KM/SEC
334 KM/SEC
356 KM/SEC
AA
DEC
330

Figure 14. Beam-smoothed radial velocity distribution of particles in Model 2. The particle distributions of Figure 12 have been scanned with a 4.4 arcmin beam as described in Figure 13.

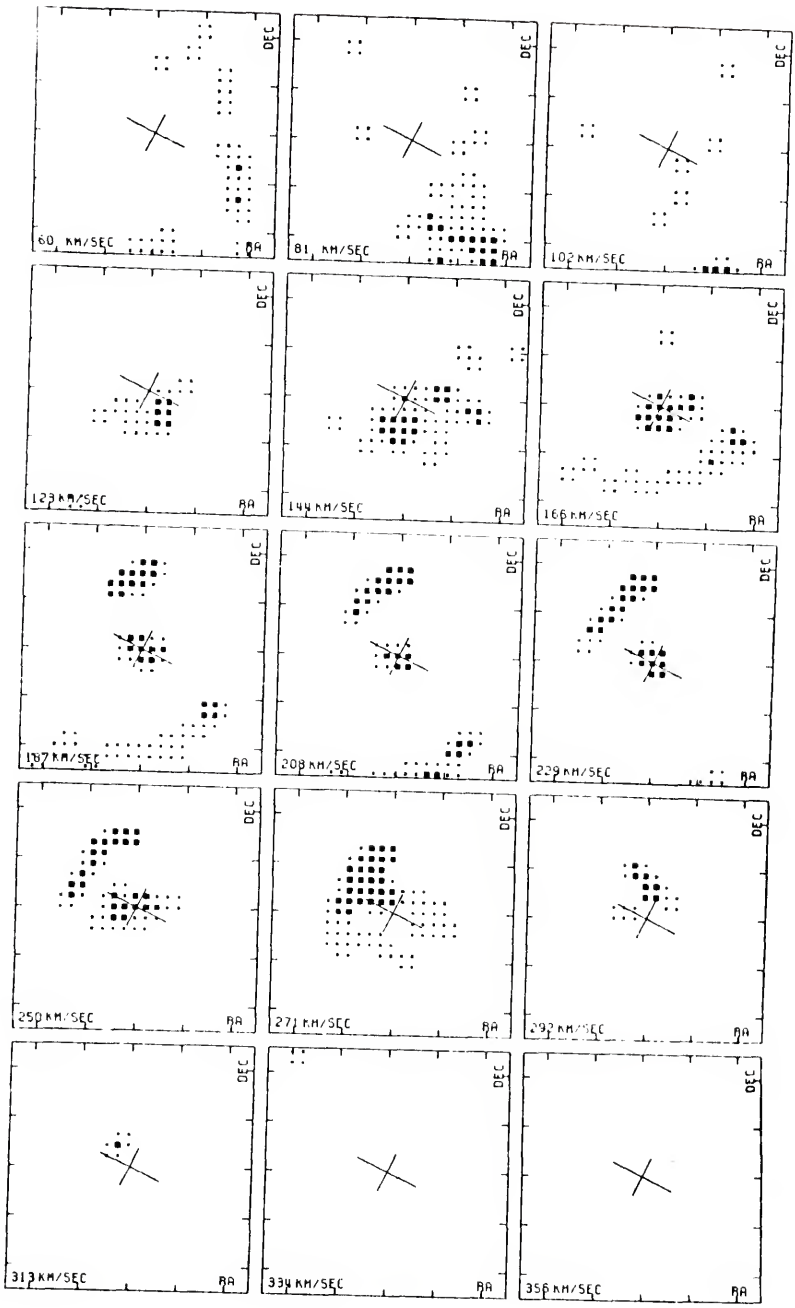
DEC
RA
60 KM/SEC
81 KM/SEC
102 KM/SEC
123 KM/SEC
144 KM/SEC
166 KM/SEC
187 KM/SEC
208 KM/SEC
229 KM/SEC
250 KM/SEC
271 KM/SEC
292 KM/SEC
313 KM/SEC
334 KM/SEC
356 KM/SEC

Above 144 km/sec the model radial velocity distributions consist primarly of particles associated with M82. One clear cut difference between the models is that Model 1 shows a definite skewing of the velocity distribution toward higher velocities, particularly in the 292 km/sec map. Comparison with the GW maps clearly shows that the radial velocity distribution of Model 2 follows the observational distribution more closely than Model 1. One feature is common to both distributions at velocities near 250 km/sec. Long chains of particles at similar velocities run northward from the major axis along the northern spike. Cotrell (1977) remarked that the isovelocity contours in this region became nearly perpendicular to the major axis with a velocity gradient nearly parallel to the minor axis, a result clearly indicated by the models.

The worst agreement in either model is in the low velocity maps. The large concentrations of material at velocities of 144 km/sec or less are conspicuously absent in the bridge. The bulk of the material at these low velocities in the models comes from the outer portions of M81. If the gas concentrations in the bridge did originate with M81, the original gas distribution in M81 must have been quite different than that assumed by this model. This point will be discussed further in Chapter V.

Perhaps the most intriguing event occurring in both models is the large amount of infall of particles from both galaxies that occurs in M82. During the course of the encounter in Model 1, 43 particles from M81 and 92 particles from M82 entered the inner 2.5 kpc of M82. In Model 2, 51 M81 particles and 92 M82 particles entered the same region. At the same time, the infall into a similar region about M81 was 2 particles for Model 1 and 1 particle for Model 2. In other words, in

both models nearly 16% of the total number of particles in both galaxies and 28% of the particles in M82 alone had trajectories that brought them into the nuclear regions of M82. The possible implications and importance of this event will also be discussed in Chapter V.

Both models follow similar evolutions after the time illustrated. The distribution around M82 continues to expand and become more diffuse. By 4 x 10^8 years after perigalacticon, the distributions increase their projected linear dimensions by nearly half. The coalescing of the M81 particles in the southwest part of that galaxy clearly evident in both models eventually forms a spiral arm-like feature that persists for a few galactic rotations.

While these final models were being perfected, studies were also performed to see the effects of changing the mass of M82, its tilt, and the position angle of its major axis. For any assumed {e, T, q} the effect of changing the mass is to change the orbital angles. In the case of the M82 direct orbits about M81 at about 2 x 10^8 years after perigalacticon, decreasing the mass increases the inclination of the orbit with respect to M81. This has an immediate adverse effect on the production of the M81 bridge. Increasing the mass has the opposite orbital effect, but the increased circular velocities of the particles in M82 due to the larger mass are immediately visible in the radial velocity field. In both cases, the positioning of the northern spike of M82 becomes more difficult. Variations of the mass of M82 of 20% and 50% were attempted. Though models were found that were similar to Models 1 and 2 for the 20% variation, the 50% mass variations produced either too high of a velocity distribution, in the case of the increased mass, or an insignificant M81 bridge, in the case of the low mass models.

The orientation of M82 in space deduced by observation seems to be consistent with the results of these models. Variations of the position angle of the major axis of up to 5 degrees produced little effect. Assuming M82 is a nearly edge on disc system, the position angle of the major axis probably can not be more than 5 degrees in error from the 64.5° measured by Heckathorn (1972). The assumed tilt of the galaxy of 10° (northwest near the observer) is close to that deduced by Lynds and Sandage (1963). Variations of this angle by 10° or more in either direction produce easily observable structural changes. The northern spike, in particular, is affected, suffering shortening and broadening by the changes in inclination.

Little direct evidence is available about the motions of the gas in the plane of the sky. However, Solinger et al. (1977) compared the distribution of light in the M82 halo to that produced by a model galaxy embedded in a dusty medium. From this analysis, they deduced that the flow of gas in the plane of the sky around M82 was about 140 km/sec southwest to northeast. Figure 14 shows the plane of the sky velocity field for Model 2, and Figure 15 illustrates the details of this field in and around M82. The magnitude and direction of the flow around M82 is quite similar to that predicted by Solinger et al. (1977).

The NGC 3077 Model

NGC 3077 proved a much more difficult object to model for several reasons. Its low systemic velocity allows solutions for ellipses, parabolas, and hyperbolas. The lack of any structural information about its orientation in space introduces the tilt and position angle of the

Figure 15. Plane of sky velocity vectors of particle distribution of Model 2 shown in Figure 10. Each vector begins at a particle and indicates the direction and scaled magnitude of that particle's motion in the plane of the sky. Vectors which would extend beyond the bounds of the plot or whose magnitudes were less than about 30 km/sec (the size of the arrow head) have been omitted from the plot. Other plotting conventions are the same as in Figure 9.

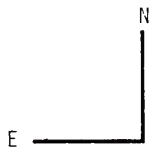

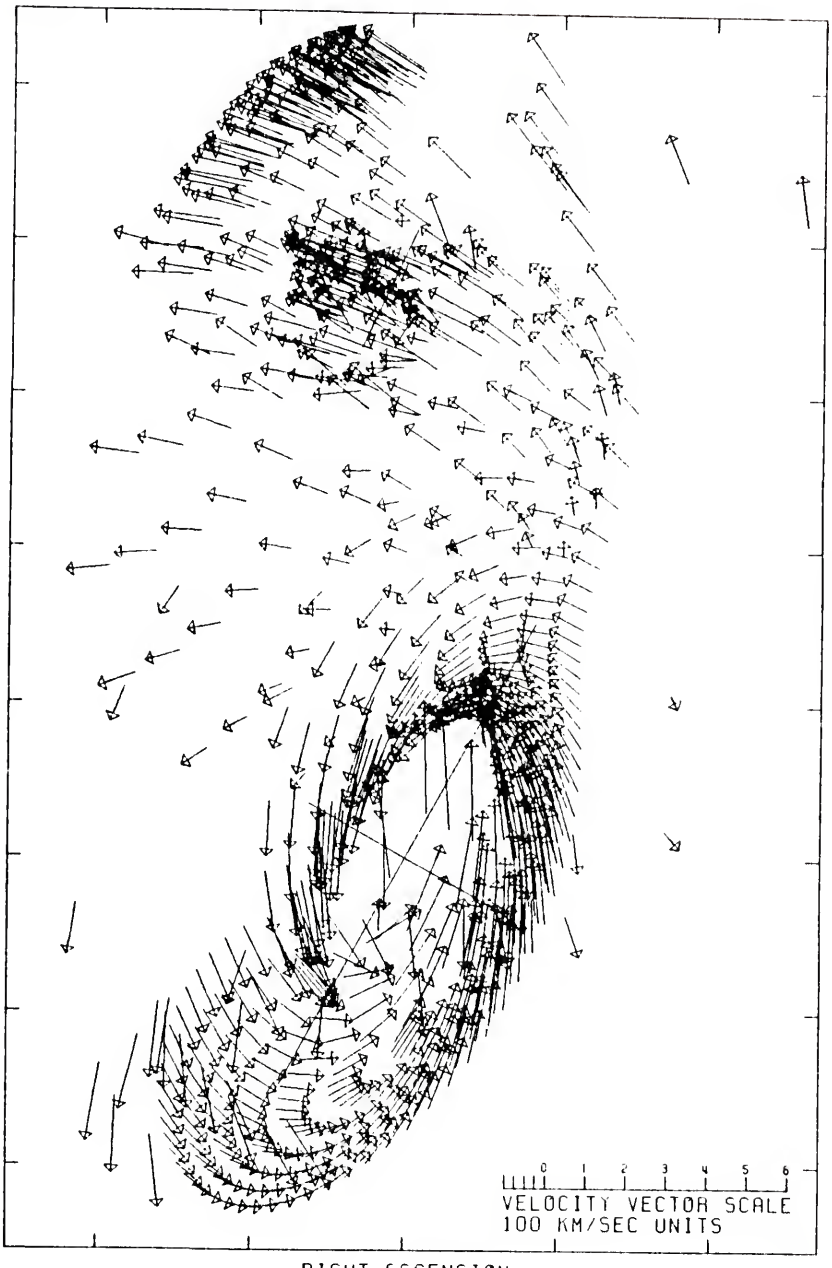
DECLINATION
0 1 2 3 4 5 6
VELOCITY VECTOR SCALE
100 KM/SEC UNITS
RIGHT ASCENSION

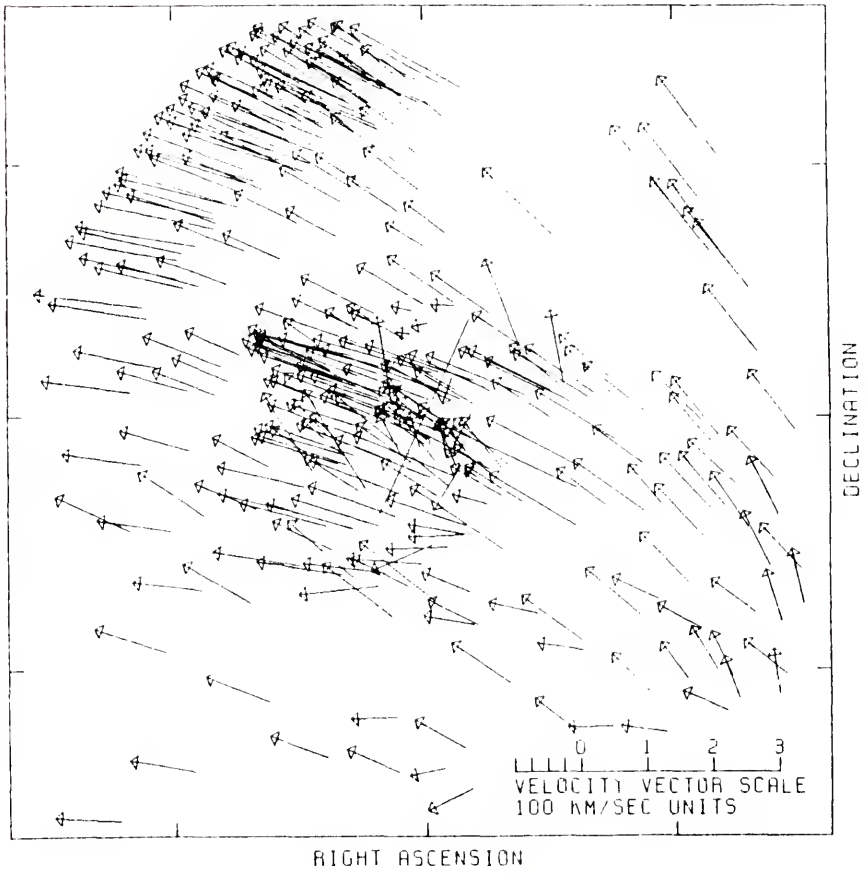

Figure 16. Detail of plane of sky velocity vectors of Figure 15 in and around M82. Cross indicates the Holmberg (1958) dimensions and assumed orientation of M82. Coordinate tic marks are at 10 arcmin intervals from M82's center.

major axis of the galaxy as two more "free" parameters to be considered. In addition, it was found that both retrograde and direct orbits of 3077 about M81 produce similar disturbances in M81 and that the slightest change in orbital parameters could drastically alter the nature of the particle distribution.

The bridge to 3077 from M81 provided a great deal of orbital and timing information. The bridge appears to be kinematically associated more closely to the material in the outer portions of M81 than to the main body of 3077 (van der Hulst 1977; hereafter denoted as vdH). Assuming that the bulk of the bridge material does come from M81, the effects of several types of 3077 passages on M81 were studied. Retrograde passages of 3077 produced only diffuse particle distributions to the east of M81; even the most destructive cases, when 3077 was nearly in the plane of M81, produced only a suggestion of a bridge feature. No retrograde orbit was found to produce a bridge of the size and extent observed by vdH.

The direct orbits were definitely favored for the production of the bridge. The geometry of the observations dictated an orbital solution with a northern perigalacticon for 3077 relative to M81 for the assumed systemic masses, relative velocity, and projected separation for times near perigalacticon. Hence, the effects of 3077's passage were to elongate the rings of test particles in the northern sections of M81 to the east, in the direction of 3077's motion. For this material to develop into the observed bridge, the time elapsed since perigalacticon had to be relatively long so that the combined effects of galactic rotation and the perturbing accelerations of 3077 could carry the particles into the region indicated by the observations. Times between 4 and 6×10^8 years after perigalacticon were found to be sufficient to

produce the bridge-like feature. At earlier times, the bridge did not extend far enough; at later times, the rotational and peculiar motions of the particles simply dispersed the bridge.

Within this time bracket, variations of the orbital parameters had a great effect on the nature and composition of the bridge. The value of q, the distance of closest approach, was still restricted to values greater than 15 kpc, as in the case of the M82 models, to preserve the M81 structure at 10 kpc. Increasing the value of q caused the bridge particles to be drawn from the more distant rings. Geometrically, increasing the value of q for a given eccentricity, lowered the plane of 3077's orbit into the plane of M81, thereby increasing the amount of destruction of M81 both by having 3077 more nearly in the plane of the particles and by lowering the velocity at which the interaction occurred. Varying the orbital eccentricity for a given q also changed the nature of the bridge geometrically. In general, the near parabolic orbits had the lowest inclinations with respect to M81's plane, thus making them the most destructive from that standpoint.

Another artifact of the production of the bridge on the eastern side of M81 was the creation of a spiral arm-like feature on the western side of the galaxy. This feature was well defined structurally from about 4×10^8 years after perigalacticon and persisted usually for a few galactic rotations. Its shape, extent, and position could also be altered by adjustment of the orbital parameters. Close passages early in the time bracket produced the arms with the greatest length and breadth in the region of the inner rings of M81. Later and/or more distant passages shortened the arm and moved it further away from the M81 nucleus. This feature is quite similar to the outer spiral arm-like

feature in M81 observed by Rotts and Shane (1975) and Gottesman and Weliachew (1975) in both shape and extent.

The interaction also perturbed a number of particles from M81 to great distances from both galaxies. Since the entire M81 system is imbedded in a neutral hydrogen cloud (Roberts 1972), at first this event might seem a possible explanation for the origin of the hydrogen envelope. However, the particles at great distances are found almost exclusively northeast of M81. Within the time bracket allowed for the development of the bridge, the model would appear to be incapable of producing the more uniform distribution observed by Roberts.

Though the prograde orbits could structurally reproduce the M81 phenomena for a wide range of orbital parameters, the reproduction of the 3077 features were much more difficult. As in the M82 models, the low mass ratio (1/10) makes the result of the interaction very severe for 3077 structurally. This problem is further complicated by the low relative velocity of the two galaxies at close approach dictated by the geometrical solutions for the orbits.

Both Cotrell (1976) and vdH found the 3077 HI structure to have a distinctive shape consisting of a spike of neutral hydrogen extending northwestward from the eastern side of the galaxy's main body. Reproduction of this spike proved to be exceedingly difficult at first. The difficulty was coupled primarily to the assumption that the major axis of the galaxy was within the range of 45° to 60° indicated by the observations of Barbieri et al. (1974) and Davies (1974). The solutions for the orbital parameters with respect to 3077, assuming the position angle was within this range, led to particle distributions which bore no

resemblance to the observations structurally. For direct passages, 3077 was elongated more or less along its major axis. These types of distributions could be broadened or narrowed by varying the tilt of the galaxy, and they could be lengthened or contracted by changing the distance of closest approach. For q values of 18 kpc or less these types of passages were catastrophic for 3077, the bulk of the material being captured in a very tight orbit about M81 or dispersed widely through the area to the east of M81. The retrograde passages with respect to 3077 produced a distorted galaxy but also failed to produce the spike.

After a wide range of tests at various values of T, e, and q within the assumed range of the position angle of the major axis of 3077, it was decided that if the spike was a result of the interaction, the orbital geometry, and hence the position angle of the major axis, must be quite different than what had heretofore been assumed. The position angle of the major axis was gradually increased, and the nature of the disturbance was observed for each new orbital geometry.

Once the position angle passed 160°, the spike feature became a natural consequence of the interaction for the direct passages for a wide range of values of q and e. Like the M82 models, its position and shape could be altered by changing the inclination of the galaxy and the orbital eccentricity. Models in this range also produced a second spike feature at nearly right angles to the first one. This new feature extended generally westward from the main body of the galaxy and into the M81 bridge. The extent, shape, and breadth of the spikes could be controlled by variation of the tilt of the galaxy, though tilts with the southeast edge of the galaxy nearest the observer were preferred for best shape control.

The geometrical constraints also appear to be quite stringent for the value of the position angle of the major axis. For example, for e = 1, q = 17.5 kpc, and T = 5 x 10^8 years after perigalacticon, if the position angle of the major axis equals 131°, 3077 is cataclysmically destroyed, while with the position angle at 161° the interaction produces the spike. The common geometrical parameters between the spike producing models seem to be the inclination of the orbit to 3077 and its respective argument of pericenter, nearly all the models which produced the spike had an orbit inclined nearly 90° to 3077 with the close approach occurring nearly in the galaxy's plane.

Since the spike occurred for such a wide range of parameters, it now became necessary not only to position the spike, but also to regulate the size of 3077. Cotrell (1977) and vdH have mapped the spike only to about 10 arcmin north of 3077. Depending on the size of the galaxy, however, the model spike could easily extend several times this length for different values of q. For example, in the q = 17.5 kpc model quoted above, a ring of radius 8.5 kpc was drawn almost 40 arcmin northward of the galaxy. Therefore, each model had a different maximum ring radius in order to maintain the 10 arcmin spike length.

Figure 17 shows a typical model particle distribution for the 3077 passage. The bridge and spike are both present, as well as the spiral feature west of M81. This model has been selected because of its structural similarity to the observations. The spike in vdH's observations is nicely centered within the model spike, and this distant passage (q = 22.5 kpc) is capable of sustaining a rather large 3077 so that the effects could be noted more easily for a moderate amount of computation. Figure 18 shows the gated radial velocity maps of this distribution. The

Figure 17. Particle distribution for M81-NGC 3077 model at 6 x 10^8 years after perigalacticon. Circles were originally about M81; 3077's particles are indicated by asterisks. The crosses indicate the Holmberg (1958) dimensions and assumed orientations of the galaxies. Coordinate tic marks are at 10 arcmin intervals from M81 center. Solid line indicates orbital path of 3077 about M81, and the arrow locates the perigalacticon with respect to the center of M81.

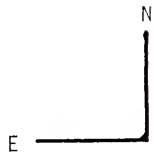

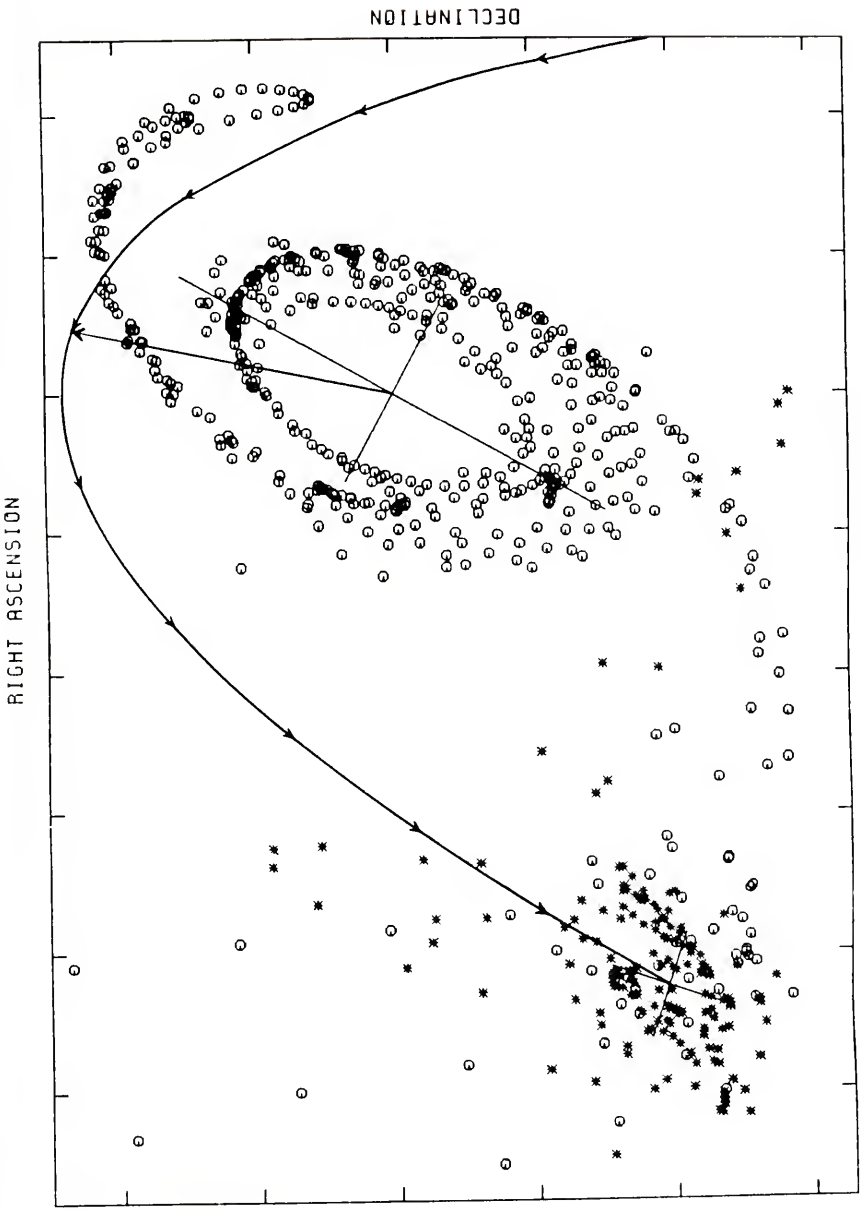
DECLINATION
RIGHT ASCENSION

Figure 18. Radial velocity distribution of particles near NGC 3077 shown in Figure 17. Particles were plotted if their radial velocities were within a 20 km/sec bandwidth centered on the velocity listed in the lower left corner of each plot. Cross indicates Holmberg (1958) dimensions and assumed orientation of 3077. Coordinate tic marks are at 10 arcmin intervals from 3077's center.

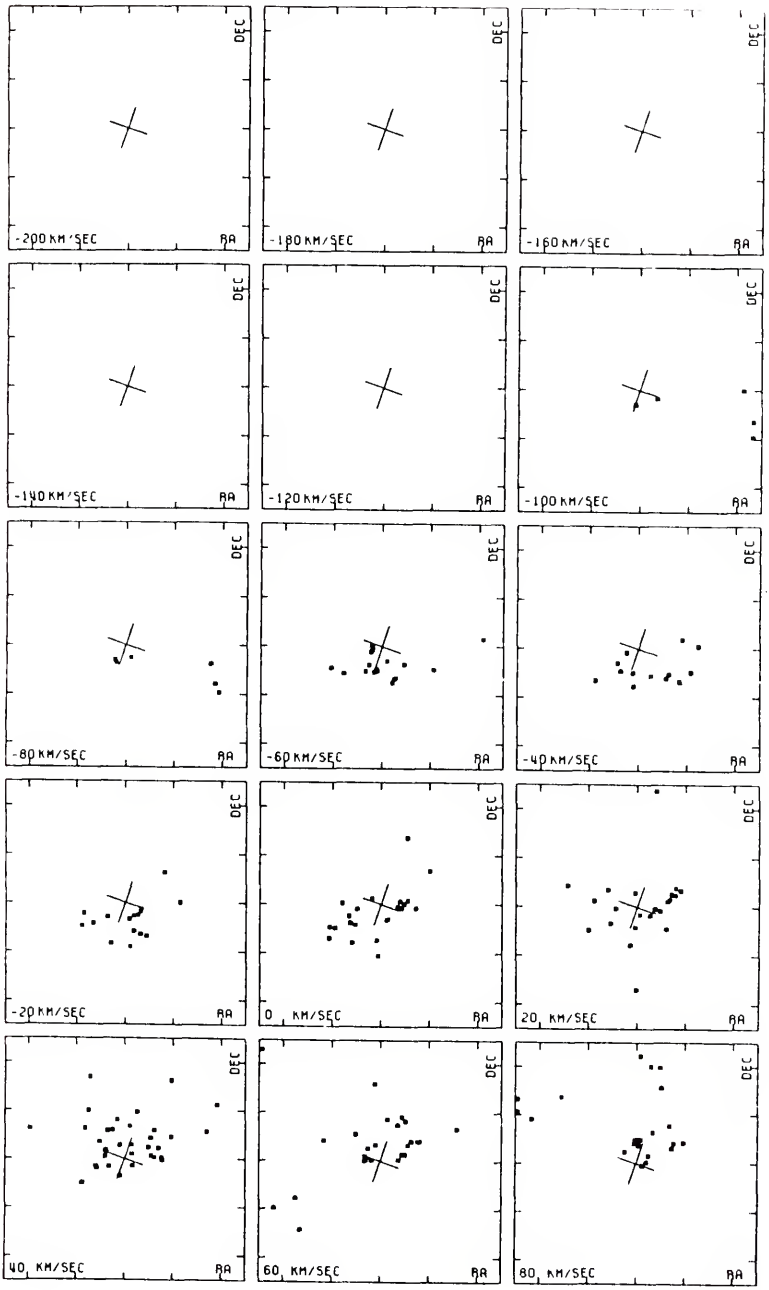
-200 KM/SEC
-180 KM/SEC
-160 KM/SEC
-140 KM/SEC
-120 KM/SEC
-100 KM/SEC
-80 KM/SEC
-60 KM/SEC
-40 KM/SEC
-20 KM/SEC
0 KM/SEC
20 KM/SEC
40 KM/SEC
60 KM/SEC
80 KM/SEC
DEC
RA

bandwidth of the gate was 20 km/sec which was centered on the radial velocities used by vdH in the construction of his single channel maps so that the model and observations can be intercompared. No beam-smoothed maps were constructed for this model since vdH's beam was approximately the size of the points plotted on the graphs.

Because of the discreteness of the model distribution, intercomparison with the high resolution observations of vdH is difficult. Structurewise, the model follows the trend of the observations well. Kinematically, the distribution of radial velocities around 3077 at small positive and negative velocities is areally similar, though the detail is missing and the distributions are somewhat broader as expected due to the coarseness of the model when compared to the observations.

Perhaps the most interesting point of this model, as in the case of the M82 models, was the large amount of particles that enter the nuclear regions. The inner 2.5 kpc of 3077 was penetrated by 65 or 42% of its own particles and 9 particles from M81. In the same time period, only 4 particles entered a similar region about M81. The importance of this event will be discussed in Chapter V.

The chief failures of this model are probably associated with M81's distribution. The model fails to produce the observed breadth and high negative velocity distribution of the bridge, and the western spiral arm is not exactly coincident with the outer spiral features of M81. Both of these problems could be model related. As previously mentioned, time, eccentricity, and distance of close approach can all affect the nature of the bridge and spiral arm. Since the M82 model proved tractable by variation of these parameters, it seems reasonable to suppose that some improvement could be gained by further modelling. Also, the inherent

discreteness of the model could be reduced by increasing the number of rings and particles at the expense of a great deal of computation time. Since the 3077 models are so sensitive to the slightest change in orbital parameters, it seems more reasonable, however, to take a model such as this one as an indicator of what is possible than to push the model to try to duplicate observations as detailed as those available for 3077.

CHAPTER V

CONCLUSIONS

The results reported in the previous chapter clearly indicate that it is possible to build models which can adequately mimic both the observed structures and radial velocity distribution in the system, particularly of the minor galaxies. If these models are similar to the actual events they are attempting to duplicate, much can be inferred about the consequences of the tidal encounters for each of the three galaxies.

Perhaps the most important consequence of the models is the large amount of infall of particles to the inner regions of the minor galaxies. Provided the gas follows similar trajectories, the central regions of both galaxies have received a large injection of gas as a result of their close approach to M81. Though the models are not strictly applicable in inner region of the galaxies, this event suggests the following scenario.

The tidal forces experienced by the minor galaxies perturbed a great quantity of gas into free fall toward the nucleus of each. This free falling material radically changed local conditions in the interstellar medium as it plunged inward. The new gas injection raised the interstellar gas density and induced shockwaves in the interstellar medium. The shockwaves compressed the enriched interstellar medium and initiated a new era of star formation. In these regions of star formation, dust also formed and was mixed into the medium by the turbulence of the gas flow.

It is not possible to estimate the mass of gas that the injection involves in the case of either of the minor galaxies. The particles which reach the nuclear regions come from many radii and do not form as a group any well defined area distribution in the original models. Hence, it is not possible to use some average HI mass surface density and area occupied by the particles to estimate the mass. However, the number density of the particles reaching this region at least indicates the relative importance of the sources of the gas. In the case of 3077, the bulk of the infalling material comes from itself. For M82, however, a significant number of the infalling particles come from M81. Since M81 is so much larger than M82, it could be that the mass contributed by M81 to the M82 nucleus is comparable to that produced by the collapse of M82 itself.

The differences between M82 and 3077 can be attributed to time and the nature of the infall. Since the model indicates that 3077 was originally somewhat smaller than M82 and that it received little material from M81, it is reasonable to suppose that total mass of the injection was small compared to that of M82. Also the time scale of the models indicates that 3077 has had much longer to recover from the effects of the interaction than M82. Any O and B stars produced by the 3077 interaction would have long since evolved away. The dust and filament structures in the galaxy (Demoulin 1969; Barbieri et al. 1974) and the stellar distribution skewed toward Population I stars of type A or later in the nuclear regions (Chromey 1974a,b) are simply the remnants of the interaction. In M82, however, the injection was both more massive and more recent according to the models. The great amount of dust and the vast number of early type stars seems to indicate that M82 has undergone a very rapid era of star formation within the last 10^8 years (O'Connell and

Mangano 1978). Since this time is comparable to the modelled time since close approach and the onset of the infall, it appears that the star and dust formation are natural consequences of the interaction.

As noted in Chapter IV, it was difficult for the M82 models to kinematically reproduce the bridge features at low velocities. This is possibly due to the fact that the M81 structure had already been significantly altered by 3077 by the time M82 reached close approach. The outer spiral arm feature of M81 produced by 3077 provides a much denser particle distribution in the region from which M82 draws the M81 bridge; hence, it is probable that the production of the M81-M82 bridge is, in detail, quite dependent on the exact time between the passages of the two galaxies and the orientation of the 3077 produced spiral feature at the time of M82's close approach.

One HI feature that the model also fails to produce is the large clump northeast of M81 observed by Gottesman and Weliachew (1975) and by Rotts and Shane (1975). This clump could have been perhaps produced by the M82 modification of the 3077 disturbance in the northern part of M81 as noted above. Kinematically, this clump has similar velocities to the 3077 features. Interestingly, if the size of the 3077 annulus is allowed to increase to the size of M82, the spike feature of the 3077 distribution extends nearly into this region. However, the observations of the region from the tip of the 3077 spike to the clump are incomplete and can not verify this possibility. Gottesman and Weliachew (1975) also pointed out that the clump was near in position to that of one of the dwarf systems, DDO 66. This companion might also be produced by the interactions, but it could be an actual satellite of M81. Since dwarf companions can be important in the development of a model (cf. Combes 1978), the possibility that this clump

and perhaps some of the others in the system are due to the dwarf systems can not be disregarded.

The models also seem to indicate that neither interaction is responsible for the large HI envelope around the system observed by Roberts (1972). Though 3077 is most successful at moving material to great distances around the galaxies it does not produce the more uniform gas distribution that is observed, nor does it appear to be capable of doing so. The periods of the near parabolic, distant passage orbits that position the spike well in the 3077 models are typically a few time 10^{10} years. Closer orbits result in the nearly complete destruction of 3077 on the first passage, making it doubtful that any HI structure would be observed at all during subsequent passages. Therefore, the models' time and structure dictate that both galaxies are going through their first close approach and are therefore incapable of producing the envelope by periodic interactions with M81. If the envelope was drawn from M81 and is not simply the natural extent of the M81 hydrogen structure, then the tidal agent which produced the envelope is not immediately obvious.

The effects of 3077 and M82 on each other are probably minimal. As pointed out by Toomre (1974) the production of bridges and tails requires a close, slow passage of unequal masses. Considering the 3077 model and Model 2 of M82, it appears unlikely that the two minor galaxies meet Toomre's conditions. Since the masses are equal, the interaction would be minimal, and even at closest approach, the galaxies are separated by approximately 65 kpc with a relative velocity of about 70 km/sec.

Model 2 of the M82 interaction seems to argue strongly for the revision of the systemic velocity of M82. The value of +210 km/sec (heliocentric) used by Model 2 is near the CO velocity field center of

symmetry determined by Rickard et al. (1977a). Since the CO observations reflect the characteristics of a normal disc system more than the hydrogen or optical emission structures do, it is probably better to use the +206 km/sec Rickard et al. (1977a) velocity as a fiducial indicator of the systemic velocity than any other available criteria in this highly disturbed system. The success of Model 2 in reproducing the Gottesman and Weliachew (1977) radial velocity field near M82 using a system velocity near this value seems to indicate that systemic velocity of M82 is at least 30 km/sec lower than the accepted value of +240 km/sec based on the work of Heckathorn (1972) and Weliachew (1974).

The only previously developed models of this system have been formulated by van der Hulst (1977). The trends of his 3077 model are quite similar to the one presented here. The M81 bridge to 3077 and the spiral arm of M81 are both produced in a similar manner to the one described in this work. His failure to find the spike distribution of 3077 can be traced to his assumed position angle of the major axis and the orbital geometry that results. His M82 model fails entirely to produce the observed distribution for M82 or the bridge. This can be traced to his assumption of a mass for M82 of 5×10^{10} solar, which the models in this work indicate is too large, and his model time of 5×10^{8} years after perigalacticon, which likewise is too long. Van der Hulst's aim with his M82 model appears to have been to increase the particle density of the bridge from M81 to 3077 by having M82 contribute its perturbations of the M81 distribution to 3077's. Though he accomplished his aim, the result was to ignore the M82 features entirely.

In summary, this work has presented possible models of the tidal interactions between M81, M82, and NGC 3077. The models indicate that

the HI bridges, but not the HI cloud in which they are immersed, are natural consequences of such an interaction. The large scale HI structures of the three galaxies are also reproducible in the context of these interactions. Kinematical comparisons with the available observations show that the models are quite similar to what is found observationally. In the case of M82, the models argue that the systemic velocity should be lowered to around +210 km/sec (heliocentric) at least. Reproduction of the 3077 structure requires the position angle of major axis to be approximately 160° with an inclination of about 40° to the line of sight (southeast nearest observer). As a result of the interactions, both minor galaxies receive a large injection of particles into the nuclear regions. If the gas in the systems followed similar trajectories, this event could have precipitated an era of rapid star formation which could be responsible for morphological changes that cause the systems to be classified as the IO-IrrII type.

Some further work could probably be done on the system of galaxies. For example, though the minor galaxies probably do not interact significantly, the simultaneous effects of 3077 and M82 on the development of the outer M81 structures are important. Adjustment of the orbital parameters of 3077 could possibly produce a more favorable bridge to M81, though intercomparison with the observations is more difficult because of the coarseness of the model when compared to the observations. However, the models produced in this work do demonstrate that the observations can be explained within the framework of a tidal interaction between the galaxies, and they do serve as fiducial indicators of the structural and morphological changes that are the result of such interaction.

APPENDIX

The analysis of the models presented in this work depends heavily on direct comparison of the models to the HI observations of the three galaxies M81, M82, and NGC 3077. This appendix contains diagrams from the observations of Gottesman and Weliachew (1977) and van der Hulst (1977) which were extensively used as comparisons for the models. Structural and radial velocity information in these diagrams will aid the readers in following the discussion in Chapters IV and V and in evaluating the models for themselves.

Figure 19. Map of the integrated HI over the M81/M82 region at 4.4 arcmin resolution by Gottesman and Weliachew (1977). The minimum contour unit is 10.8×10^{19} atoms cm^{-3} on the sky. The dashed contours indicate regions of higher intensity than might be indicated by the cross-hatching. The coordinate system is with respect to the center of M81. This figure was reproduced by permission of Drs. S.T. Gottesman and L. Weliachew and The Astrophysical Journal.

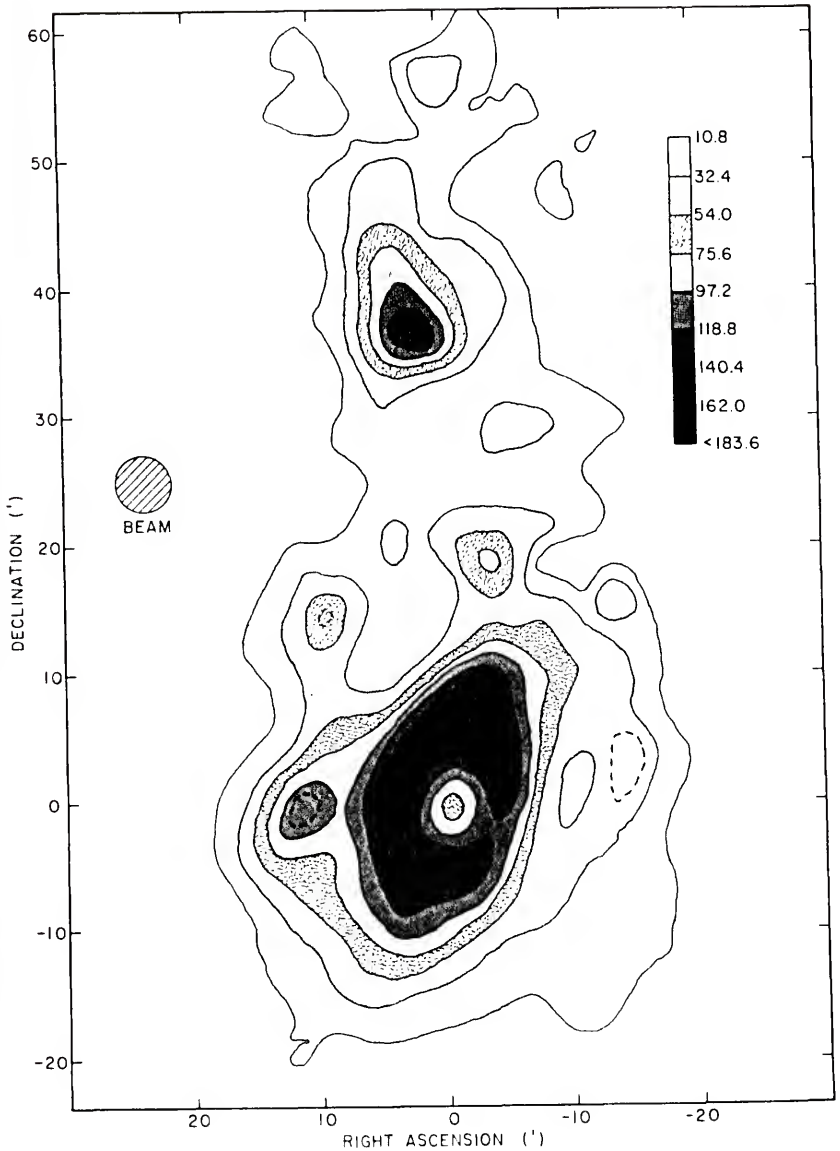
10.8
32.4
54.0
75.6
97.2
118.8
140.4
162.0
<183.6
BEAM
DECLINATION (')
RIGHT ASCENSION (')
60
50
40
30
20
10
0
-10
-20
20
10
0
-10
-20

Figure 20. Brightness temperature maps of the neutral hydrogen near M82 at different velocities with a 4.4 arcmin resolution and 21 km/sec velocity resolution by Gottesman and Weliachew (1977). The size of the cross at the center of the field is close to the optical center of M82 and is equal to the synthesized beam at half power. The oblique line drawn through the center is the Holmberg size of M82 at the assumed position angle of the major axis. The angular scale is given by the first map. The contour unit is 0.5 K, and the lowest contour level is 0.5 K except when indicated (in K). The full contours are above 3σ, and the dashed contours are between 2 and 3σ. The velocities in km/sec are indicated in the bottom left corners of the maps. This figure was reproduced by permission of Drs. S.T. Gottesman and L. Weliachew and The Astrophysical Journal.

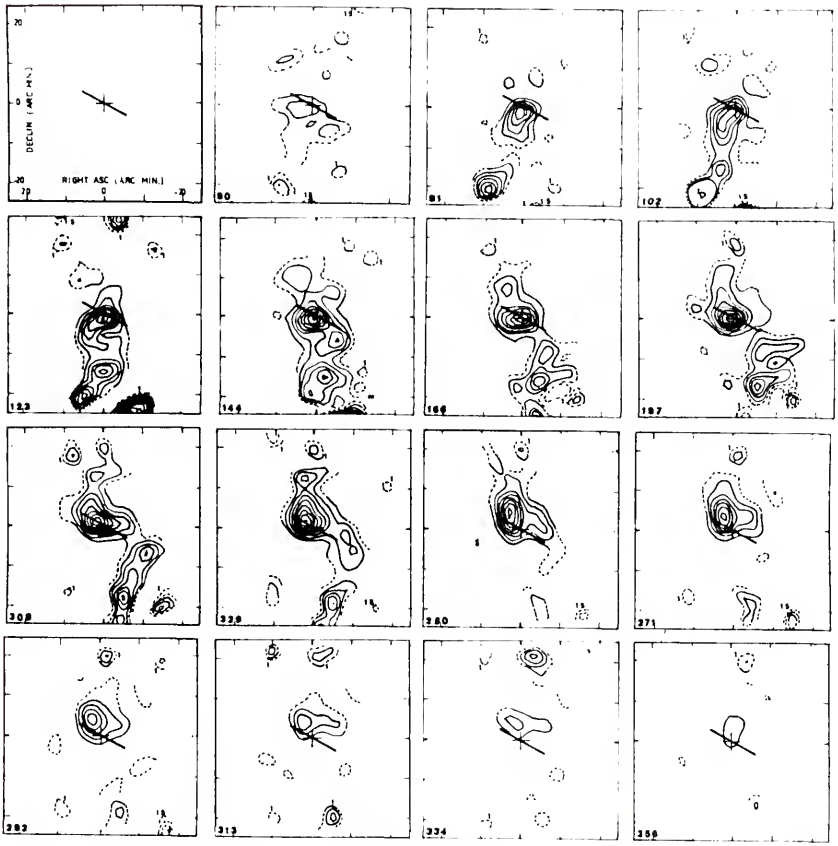
DECLIN (ARC MIN.)
RIGHT ASC (ARC MIN.)
80
81
102
123
144
166
187
208
229
250
271
292
313
334
356

Figure 21. Radiograph of the distribution of HI column density in NGC 3077 and M81 at 50 arcsec resolution. The map is a combination of the data of Rotts and Shane (1975) and van der Hulst (1977), and it has the radial velocity field of both studies superimposed on the HI distribution. The black crosses indicate the positions of the nuclei of the galaxies. The grey scale in the upper left-hand corner relates photographic density to the HI column density in units of 10 atoms/cm^2. The sharp boundary at $\alpha = 9^h53^m$ is due to the observational and reduction differences in the two sets of data. The empty regions in the upper left and lower right were not observed. The size of the 50 arcsec beam is shown in the lower right corner. This photograph was reproduced by permission of Dr. J. van der Hulst.

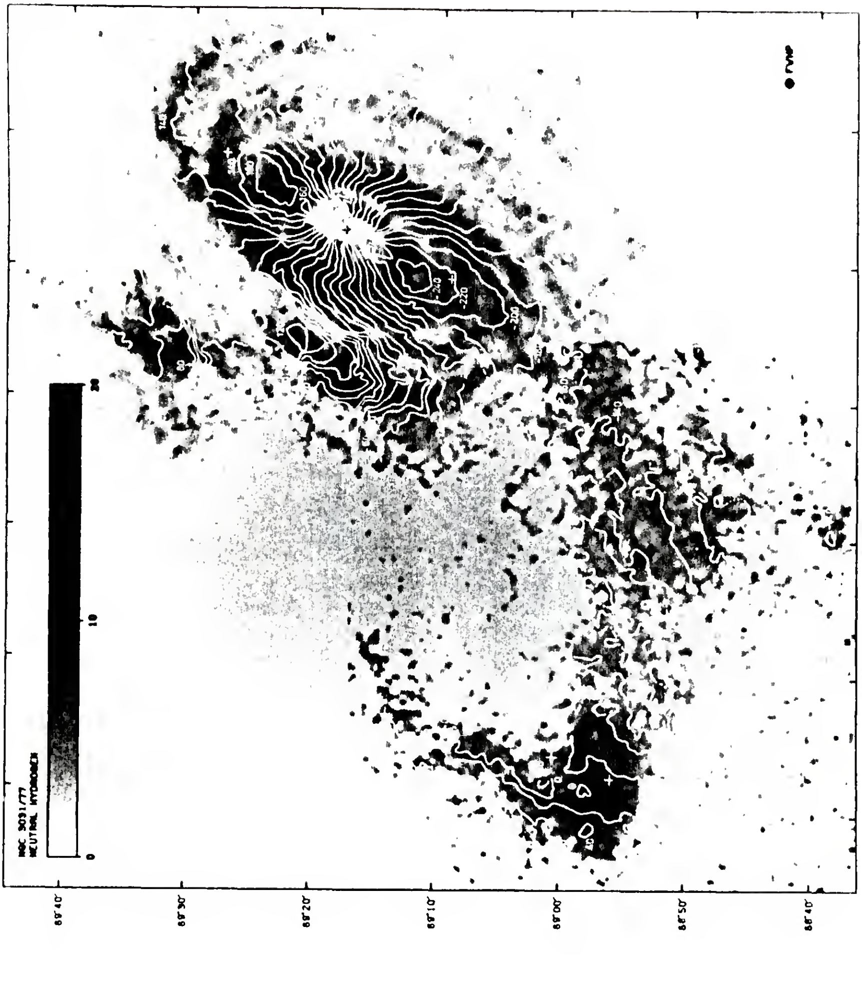
NGC 3031/77
NEUTRAL HYDROGEN

Figure 22. Contour maps of the HI line emission at different velocities near NGC 3077 by van der Hulst (1977). The contour interval plotted is 0.9 K which is twice the r.m.s. noise level. Negative contours are dashed, and the zero contour has been omitted. The radial velocities in km/sec are given in the lower right corner of each map. The half power, 50 arcsec beam width is illustrated in the lower left corner of the +80 km/sec map. The star indicates the field center, and the crosses indicate the nuclei of the galaxies. Readers should be aware of the changes in the right ascension scale of these diagrams. The first six diagrams cover the M81 bridge; the remainder cover the area about 3077. This photograph was reproduced by permission of Dr. J. van der Hulst.

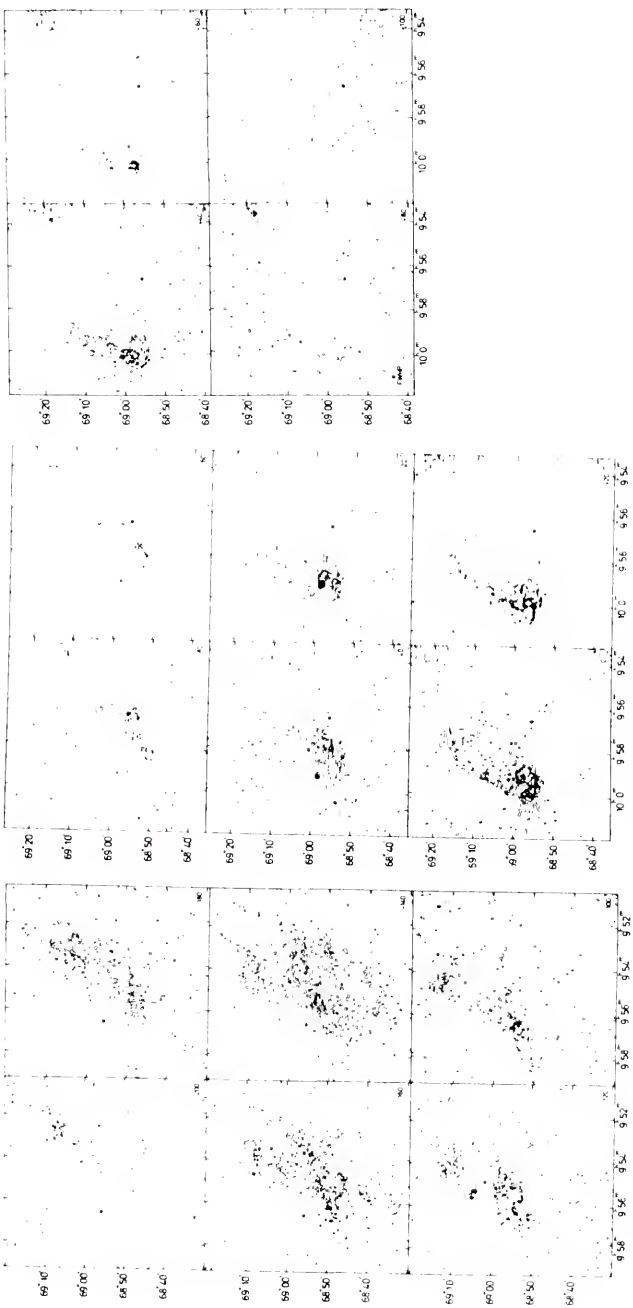

BIBLIOGRAPHY

Barbieri, C., Bertola, F., and di Tullio, G. 1974, Astr. & Astrophys., 35, 463.

Bertola, F., and Maffei, P. 1974, Astr. & Astrophys., 32, 117.

Brandt, J.C., Kalinowski, J.K., and Roosen, R.G. 1972., Ap. J. Sup., 24, 421.

Burbidge, E.M. 1968, A.J., 73, 890.

Burbidge, E.M., Burbidge, G.R., and Rubin, V.C. 1964, Ap. J., 140, 942.

Chromey, F.R. 1974a, Astr. & Astrophys., 31, 165.

Chromey, F.R. 1974b, Astr. & Astrophys., 37, 7.

Clutton-Brock, M. 1972, Astrophys. & Space Sci., 17, 292.

Combes, F. 1978, Astr. & Astrophys., 65, 47.

Cotrell, G.A. 1976, Mon. Not. Roy. Astr. Soc., 174, 455.

Cotrell, G.A. 1977, Mon. Not. Roy. Astr. Soc., 178, 577.

Crane, P.C., Guiffrida, T.S., and Carlson, J.B. 1976, Ap. J. (Let.), 203, L113.

Danby, J.M.A. 1962, Fundamentals of Celestial Mechanics (New York: The Macmillan Co.).

Davies, R.D. 1974, in IAU Symposium #58, The Formation and Dynamics of Galaxies, ed. J.R. Shakeshaft (Boston: D. Reidel Publishing Co.), 119.

De Bruyn, A.G., Crane, P.C., Price, R.M., and Carlson, J.B. 1976, Astr. & Astrophys., 46, 243.

Demoulin, M.H. 1969, Ap. J., 157, 81

De Vaucouleurs, G. 1959, in Handbuch der Physik, Astrophysics IV: Stellar Systems, ed. S. Flugge (Berlin: Springer-Verlag), 311.

De Vaucouleurs, G. 1961, Ap. J. Sup., 5, 233.

De Vaucouleurs, G. 1975, in Stars and Stellar Systems IX: Galaxies and the Universe, ed. A. Sandage, M. Sandage, and J. Kristian (Chicago: University of Chicago Press), 557.

De Vaucouleurs, G. and de Vaucouleurs, A. 1964, Reference Catalog of Bright Galaxies (University of Texas Press).

Elvius, A. 1972, Astr. & Astrophys., 19, 193.

Elvius, A. and Hall, J.S. 1962, A.J., 67, 271.

Eneev, T.M., Kozlov, N.N., and Sunyaev, R.A. 1973, Astr. & Astrophys., 22, 41.

Geldzahler, B.J., Kellerman, K.I., Shaffer, D.B., and Clark, B.G. 1977, Ap. J. (Let.), 215, L5.

Goad, J.W. 1976, Ap. J. Sup., 32, 89.

Gottesman, S.T. and Weliachew, L. 1975, Ap. J., 195, 23.

Gottesman, S.T. and Weliachew, L. 1977, Ap. J., 211, 47.

Guelin, M. and Weliachew, L. 1970, Astr. & Astrophys., 9, 155.

Hargrave, P.J. 1974, Mon. Not. Roy. Astr. Soc., 168, 491.

Harper, D.A. and Low, F.J. 1973, Ap. J. (Let.), 182, L89.

Heckathorn, H. 1972, Ap. J., 173, 501.

Holmberg, F. 1958, Medd. Lunds Astr. Obs., Ser. 2, No. 136.

Humason, M.L., Mayall, N.U., and Sandage, A.R. 1956, A.J., 61, 97.

Kellerman, K.I., Shaffer, D.B., Pauliny-Toth, I.I.K., Preuss, E., and Witzel, A. 1976, Ap. J. (Let.), 210, L121.

Killian, D.J. and Gottesman, S.T. 1977, Bul. Am. Astr. Soc., 9, 364.

Kleinman, D.E. and Low, F. 1970a, Ap. J. (Let.), 159, L165.

Kleinman, D.E. and Low, F. 1970b, Ap. J. (Let.), 161, L203.

Krienke, O.K. and Hodge, P.W. 1974, A.J., 79, 1242.

Kronberg, P.P. and Wilkinson, P.N. 1975, Ap. J., 200, 430.

Lewis, B.M. and Davies, R.D. 1973, Mon. Not. Roy. Astr. Soc., 165, 213.

Lynds, C.R. 1961, Ap. J., 134, 659.

Lynds, C.R. and Sandage, A.R. 1963, Ap. J., 137, 1005.

Mayall, N.U. 1960, Ann. d'Ap., 23, 344.

Morgan, W.W. 1958, PASP, 70, 364.

Morgan, W.W. and Mayall, N.U. 1957, PASP, 69, 291.

Morgan, W.W. and Mayall, N.U. 1959, Science, 130, 1421.

O'Connell, R.W. and Mangano, J.J. 1978, Ap. J., 221, 62.

Peimbert, M. and Spinrad, H. 1970, Ap. J., 160, 429.

Pfleiderer, J. 1963, Zeit. fur Astrophys., 58, 12.

Pfleiderer, J. and Siedentopf, H. 1961, Zeit. fur Astrophys., 51, 201.

Rickard, L.J., Palmer, P., Morris, M., Turner, B.E., and Zuckerman, B. 1977a, Ap. J., 213, 673.

Rickard, L.J., Palmer, P., Morris, M., Turner, B.E., and Zuckerman, B. 1977b, Ap. J., 214, 390.

Rieu, N.Q., Mebold, U., Winnberg, A., Guibert, J., and Booth, R. 1976, Astr. & Astrophys., 52, 467.

Roberts, M.S. 1972, in IAU Symposium #44: External Galaxies and Quasi-Stellar Objects, ed. D.S. Evans (Dordrecht, Holland: D. Reidel Publishing Co.), 12.

Rotts, A.H. 1975, Astr. & Atrophys., 45, 43.

Rotts, A.H. and Shane, W.W. 1975, Astr. & Astrophys., 45, 25.

Sandage, A. 1961, The Hubble Atlas of Galaxies (Washington, D.C.: Carnegie Institution of Washington).

Sandage, A. and Visvanathan, N. 1969, Ap. J., 157, 1065.

Sanders, R.H. and Balamore, D.S. 1971, Ap. J., 166, 7.

Schmidt, G.D., Angel, J.R.P., and Cromwell, R.H. 1976, Ap. J., 206, 888.

Seyfert, C.K. 1943, Ap. J., 97, 28.

Smart, W.M. 1965, Spherical Astronomy (Cambridge: Cambridge University Press).

Solinger, A.B. 1969, Ap. J., 155, 403.

Solinger, A.B. and Markert, T. 1975, Ap. J., 197, 309.

Solinger, A.B., Morrison, P., and Markert, T. 1977, Ap. J., 211, 707.

Szebehely, V. 1967, Theory of Orbits: The Restricted Problem of Three Bodies (New York: Academic Press, Inc.).

Tammann, G.A. and Sandage, A. 1968, Ap. J., 151, 825.

Tashpulatov, N. 1970a, Soviet AJ, 13, 968.

Tashpulatov, N. 1970b, Soviet AJ, 14, 227.

Toomre, A. 1974, in IAU Symposium #58: The Formation and Dynamics of Galaxies, ed. J.R. Shakeshaft (Boston: D. Reidel Publishing Co.), 347.

Toomre, A. and Toomre, J. 1972, Ap. J., 178, 623.

Van den Bergh, S. 1971, Astr. and Astrophys., 12, 474.

Van den Bergh, S. 1976, Ap. J., 206, 883.

Van der Hulst, J.M. 1977, doctoral thesis, Rijksuniversiteit te Groningen.

Van der Kruit, P.C. 1971, Astr. & Astrophys., 15, 110.

Van der Kruit, P.C. 1973, Astr. & Astrophys., 29, 231.

Visvanathan, N. and Sandage, A.R. 1972, Ap. J., 176, 57.

Volders, L. and Hogbom, J.A. 1961, Bul. Astr. Inst. Netherlands, 15, 307.

Von Kap-herr, A., Jones, B.B., and Wielebinski, R. 1975, Astr. & Astrophys., 41, 115.

Weliachew, L. 1974, Ap. J., 191, 639.

Wilkinson, P.N. 1971, Mon. Not. Roy. Astr. Soc., 154, 1P.

Wright, A.E. 1972, Mon. Not. Roy. Astr. Soc., 157, 309.

Yabushita, S. 1971, Mon. Not. Roy. Astr. Soc., 153, 97.

Yabushita, S. 1977, Mon. Not. Roy. Astr. Soc., 178, 289.

BIOGRAPHICAL SKETCH

David John Killian was born 19 December 1951, in Maryville, Missouri. He is the son of Stearl Bishop Killian and Agnes Elizabeth Howington Killian, and has one younger brother, Stephen Lynn, and one older step-sister, Jesse Mae Borchardt.

David was raised in the small agricultural community of Maitland in northwestern Missouri. He attended Maitland Elementary School and Nodaway-Holt High School, from which he graduated as valedictorian of his class in 1969. He then entered Northwest Missouri State University at Maryville, Missouri, where be obtained a Bachelor of Science in physics with highest honors in 1973. Also during his undergraduate career, he attended the University of Missouri-Columbia while participating in the NSF Summer Undergraduate Research Program.

In September of 1973, David entered graduate school at the University of Florida on an Arts and Sciences Graduate Fellowship. He served subsequently as a Graduate Teaching Assistant in the University of Florida astronomy laboratories while working toward his Ph.D. in astronomy. Concurrently with his academic endeavors, David developed an interest in karate and received his first degree black belt from the Cuong Nhu Karate Association in May of 1978. Upon completion of his degree, David hopes to pursue a course of theoretical and observational research in astronomy and to eventually obtain a university level teaching position in astronomy.

I certify that I have read this study and that in my opinion it conforms to acceptable standards of scholarly presentation and is fully adequate, in scope and quality, as a dissertation for the degree of Doctor of Philosophy.

Stephen T. Gottesman, Chairman
Associate Professor of Astronomy

I certify that I have read this study and that in my opinion it conforms to acceptable standards of scholarly presentation and is fully adequate, in scope and quality, as a dissertation for the degree of Doctor of Philosophy.

Carol C. Williams
Associate Professor of Astronomy

I certify that I have read this study and that in my opinion it conforms to acceptable standards of scholarly presentation and is fully adequate, in scope and quality, as a dissertation for the degree of Doctor of Philosophy.

John P. Oliver
Associate Professor of Astronomy

I certify that I have read this study and that in my opinion it conforms to acceptable standards of scholarly presentation and is fully adequate, in scope and quality, as a dissertation for the degree of Doctor of Philosophy.

Thomas L. Bailey
Professor of Physics and Electrical Engineering

I certify that I have read this study and that in my opinion it conforms to acceptable standards of scholarly presentation and is fully adequate, in scope and quality, as a dissertation for the degree of Doctor of Philosophy.

Charles F. Hooper, Jr.
Professor of Physics

This dissertation was submitted to the Graduate Faculty of the Department of Physics and Astronomy in the College of Arts and Sciences and to the Graduate Council, and was accepted as partial fulfillment of the requirements for the degree of Doctor of Philosophy.

August 1978

Dean, Graduate School